

Supplementary Information of A multitechnique approach to unveil redox behaviour and potentiality of homoleptic Cu^I complexes based on substituted bipyridine ligands in oxygenation reactions.

Barbara Centrella,^{a,†} Gabriele Deplano,^{a, †} Alessandro Damin,^a Matteo Signorile,^a Mariagrazia Tortora,^b Claudia Barolo,^{a,c} Matteo Bonomo^{a,*} and Silvia Bordiga^{a,*}

^a Dept. of Chemistry and NIS Interdepartmental Center, University of Turin, via Pietro Giuria 7, I-10125 Turin (Italy).

^b AREA SCIENCE PARK, Padriciano, 99, 34149 Trieste, Italy and Elettra-Sincrotrone Trieste, S.S. 114 km 163.5, Basovizza, 34149, Trieste, Italy

^c ICxT Interdepartmental Centre, Università degli Studi di Torino, Lungo Dora Siena 100, 10153 Torino (Italy)

[†] These two authors equally contribute to the work

To whom correspondence should be addressed: matteo.bonomo@unito.it ; silvia.bordiga@unito.it

Figure S1. Digital photograph of complexes dissolved in ACN.....	S3
Table S1. Figures of merit extracted from DFT calculations	S4
Figure S2. Cyclic Voltammograms of pristine and oxidized CuBPD	S5
Figure S3. Computed and experimental UV-Vis spectra for BPA and Cu-BPA.....	S6
Figure S4. Comparison between computed and experimental UV-Vis spectra of Cu^I and Cu^{II} complexes...S7	
Figure S5. DFT Structures of (Cu^I)⁺ and (Cu^{II})²⁺ complexes.....	S8
Figure S6. NTO analyses Cu(I)BPA.....	S9
Figure S7. UV-Vis Spectra of pristine and oxidized ligands.....	S10
Figure S8. Digital photograph of pristine and oxidized complexes in DCM.....	S11
Figure S9. Computed and experimental Raman spectra for BPA and Cu-BPA.....	S12
Figure S10. Comparison between computed and experimental Raman spectra of Cu^{I/II} complexes.....	S13
Figure S11. Full set of Raman Spectra of Cu^I complexes.....	S14
Figure S12. Raman spectra of pristine and oxidized CuBPA	S17
Figure S13. Evolution of CVs of CuBPA after the addition of oxidant and then reductant	S18
Table S2. Literature examples of (TD-)DFT studies involving Cu-complexes with oxygenated species.....	S18
Scheme S1. Reactions considered in the calculation of formation energies for CuBPA-O_x	S19
Table S3. Geometrical parameters extracted form the calculation for CuBPA-O_x	S19
Figure S14. Computed UV-Vis and Raman spectra for Cu^{I/II}-BPA, also bearing Cu-O_x species.....	S20
Figure S15. Correlation between Δv₁ and ionic radius of some metals.....	S21
Figure S16. Evolution of UV-Vis-NIR Spectrum of CuBPA after the addition of oxidant and reductant....S22	
Figure S17. GC-MS spectra of CuBPA, tBuOOH and cyclohexene.....	S23
Figure S18. GC-MS spectra.....	S24
Figure S20-21. NMR spectra of CuBPX complexe.....	S25
Figure S22. Custom-made experimental set-up employed to perform single (top) and simultaneous (bottom) spectroscopic measurements.....	S30
Appendix 1. Optimized DFT structures.....	S31



Figure S1. Different samples (CuBPA, CuBPB, CuPBC and CuBPD from right to left) dissolved in ACN. Sample concentration: 1 mM.

Table S1. Average Cu-N distance ($\langle d_{\text{Cu-N}} \rangle$, in Å), angle among the planes defined by the aromatic systems of each bpy ligand (τ , in °), Mulliken spin densities on Cu (P_{Cu}) and the oxidation potential for the $\text{Cu(I)BPX} \rightarrow \text{Cu(II)BPX}$ electrochemical oxidation (E , expressed both vs $\text{Fc}/\text{Fc}^\cdot$ and Ag/AgCl , in mV).

Model	$\langle d_{\text{Cu-N}} \rangle^a$	τ	P_{Cu}	$E_{\text{Cu(II)}/\text{Cu(I)}}$ (vs $\text{Fc}/\text{Fc}^\cdot$)	$E_{\text{Cu(II)}/\text{Cu(I)}}$ (vs Ag/AgCl)
Cu(I)BPA	2.050	88.3	0.000	275	785
Cu(II)BPA	1.999	65.7	0.625		
Cu(I)BPB	2.064	86.1	0.000	-219	291
Cu(II)BPB	2.003	41.8	0.587		
Cu(I)BPC	2.070	86.9	0.000	-96	414
Cu(II)BPC	2.005	53.3	0.632		
Cu(I)BPD	2.063	86.5	0.000	-107	403
Cu(II)BPD	2.003	42.2	0.590		

^a standard deviation is not reported since all Cu-N distances are identical

All complexes present closely monodispersed Cu-N distances that shorten upon oxidation for all models. A more remarkable structural variation caused by oxidation is the decrease in the angle τ between the two planes defined by the aromatic system of each of the bpy ligands. Such angle approaches 90° in the Cu(I) form of the complexes, i.e. the bpy ligands are oriented perpendicularly and coordinate the Cu(I) centre with closely tetrahedral geometry. Upon oxidation, τ decreases for all complexes, up to an extent dictated by the steric hindrance imposed by the (eventual) substituents of bpys. Accordingly, the magnitude of the τ variation follows the CuBPB > CuBPD > CuBPC > CuBPA ordering. This behaviour is consistent with the distortion of complexes toward the square planar coordination of Cu(II), as commonly observed for this metal cation. The oxidation potential for the electrochemical oxidation of each complex from its Cu(I) to the Cu(II) one was computed. In detail, the oxidation potential was computed against the ferrocene/ferrocenium ($\text{Fc}/\text{Fc}^\cdot$) couple, according to the following reaction:



The ΔG for the reaction was calculated accounting on the G values obtained for the isolated as a result of the thermodynamic analysis of the simulated vibrational properties of the materials, i.e.:

$$\Delta G = G_{\text{Cu(II)BPX}} + G_{\text{Fc}} - G_{\text{Cu(I)BPX}} - G_{\text{Fc}^\cdot} \quad (\text{with X = A, B, C or D})$$

Fc and Fc^\cdot structures were optimized and adopted in a frequency calculation, both performed at the same level of theory as for the CuBPX complexes (see the Computational Details section in the main text). The ΔG was converted to the oxidation potential E through the relation:

$$\Delta G = - nFE$$

The potential vs the Ag/AgCl reference electrode was finally obtained with the opportune conversion factor (+510 mV vs $\text{Fc}/\text{Fc}^\cdot$). Interestingly, the oxidation potential correlates with the variation of τ , i.e. the lower the potential, the higher the angular displacement.

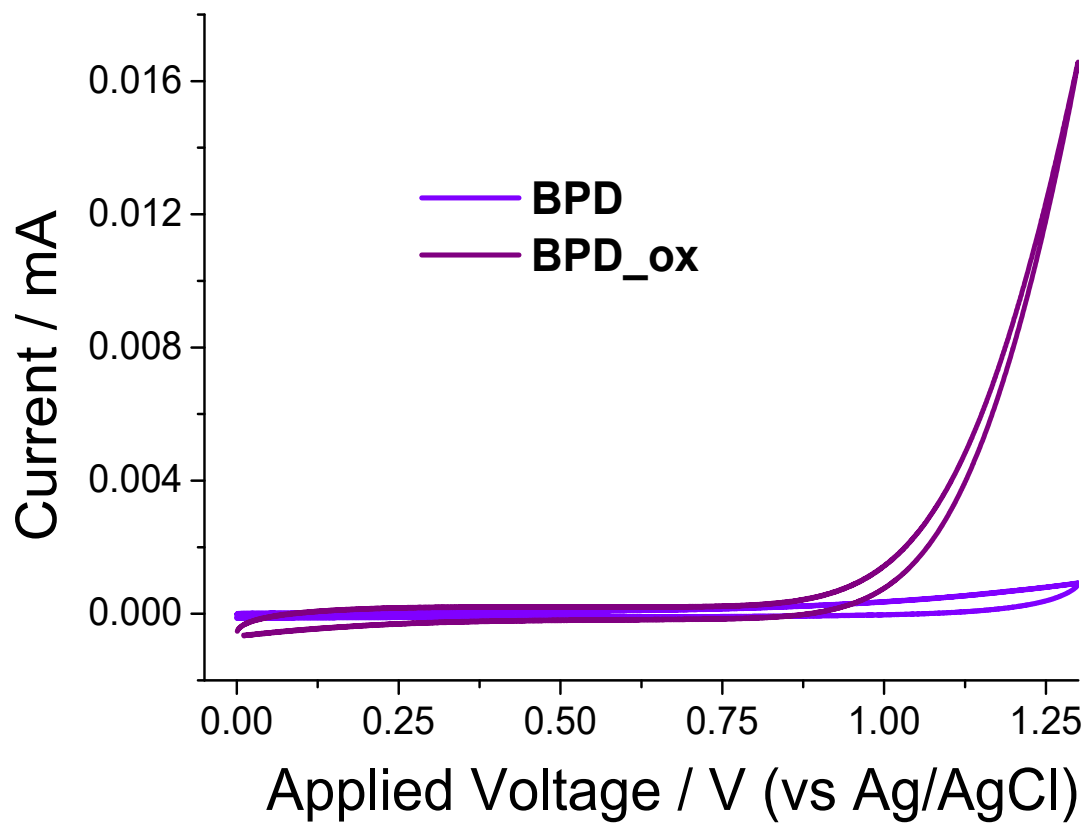


Figure S2. Cyclic voltammograms of pristine ligands (darker lines) and after 50 cycles from the addition of tBuOOH as oxidant (lighter lines) for BPD

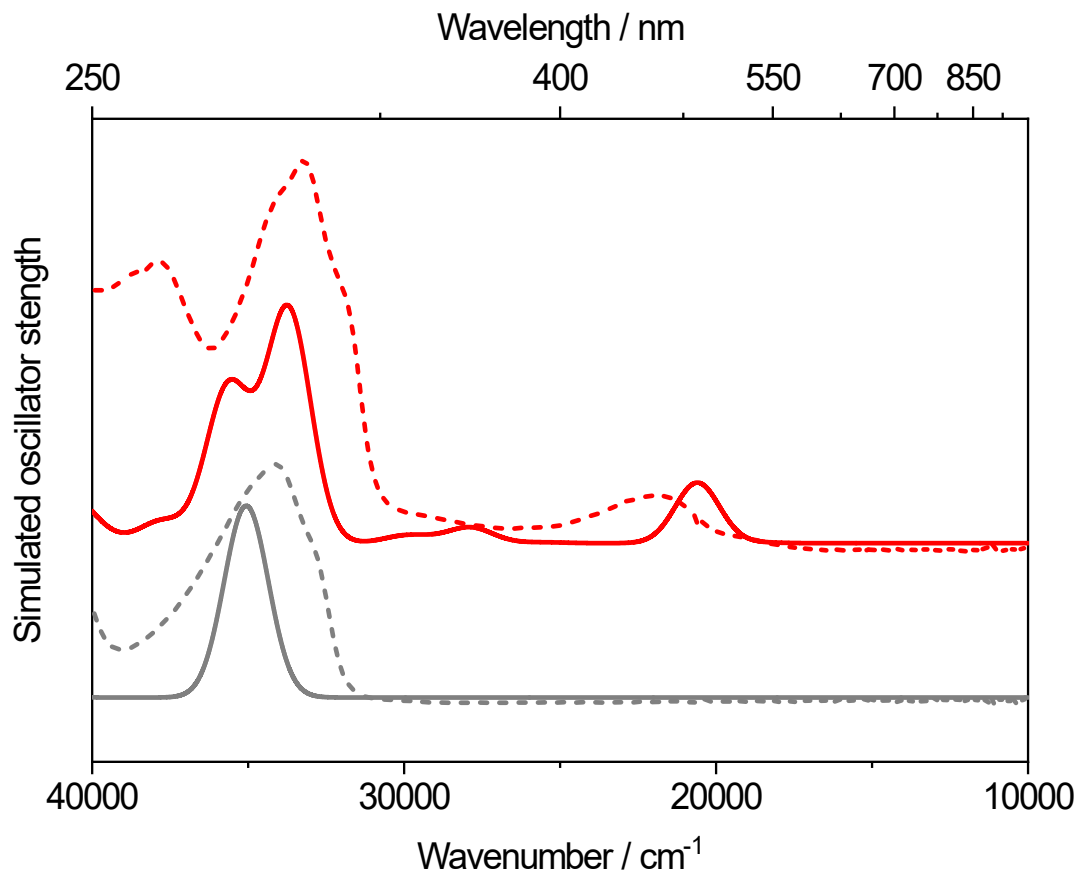


Figure S3. Computed (solid lines) UV-Vis spectra vs experimental ones (dashed lines) for Cu-BPA (ligand, in grey, and complex, in red).

With respect to the electronic transitions, the UV-Vis spectrum of Cu-BPA is quite similar to that of the pristine ligand. At higher energy, among 30000 and 40000 cm⁻¹, another intense and complex signal is observed. The structuring of the peak suggests it is the convolution of multiple bands, whose nature is inferred on the basis of NTO (*vide infra*). The electronic transition falling at 33700 cm⁻¹ in the simulated spectrum of Cu-BPA, representative for the low-energy bound of the signal, is related to a $\pi-\pi^*$ transition, *i.e.* involving the sole ligand.

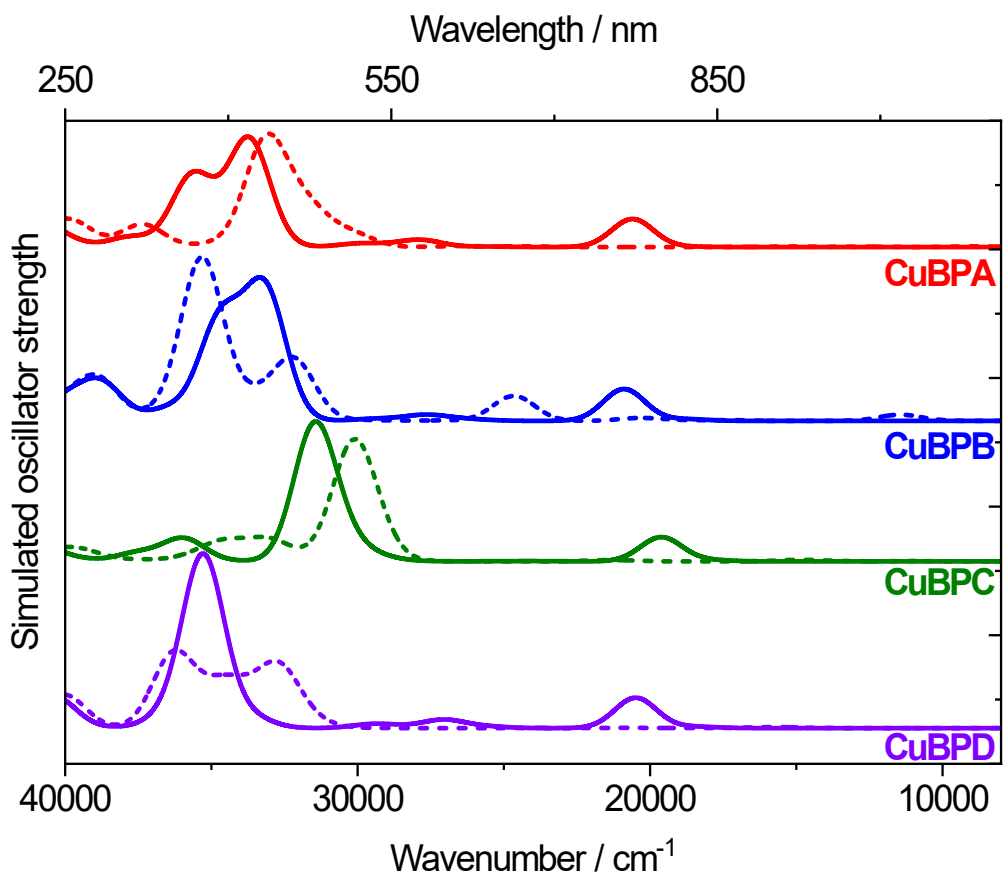


Figure S4. Computed UV-Vis spectra for all Cu complexes in Cu^I (solid lines) and Cu^{II} (dashed lines) forms. Simulated spectra have been convoluted with Gaussian functions (FWMH set to 1000 cm⁻¹ for UV-Vis).

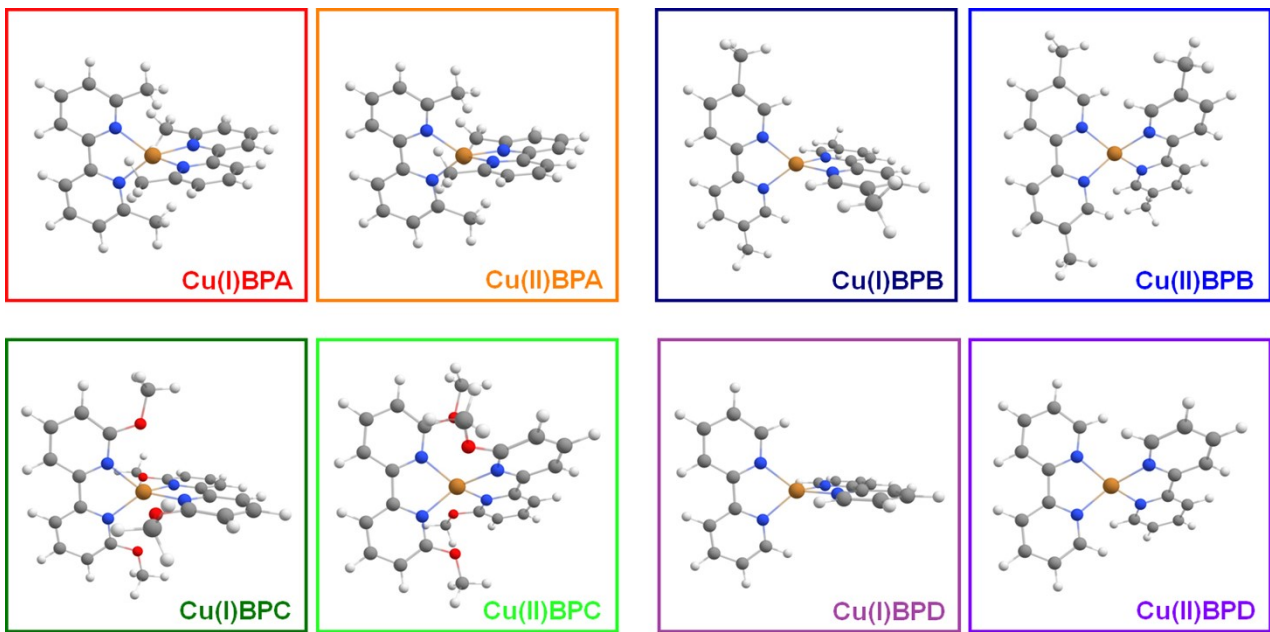


Figure S5. Optimized DFT structures of bipyridyl-based complexes in both pristine ($\text{Cu}^{\text{I}}\text{+}$) and electronically oxidized ($\text{Cu}^{\text{II}}\text{2+}$) form.

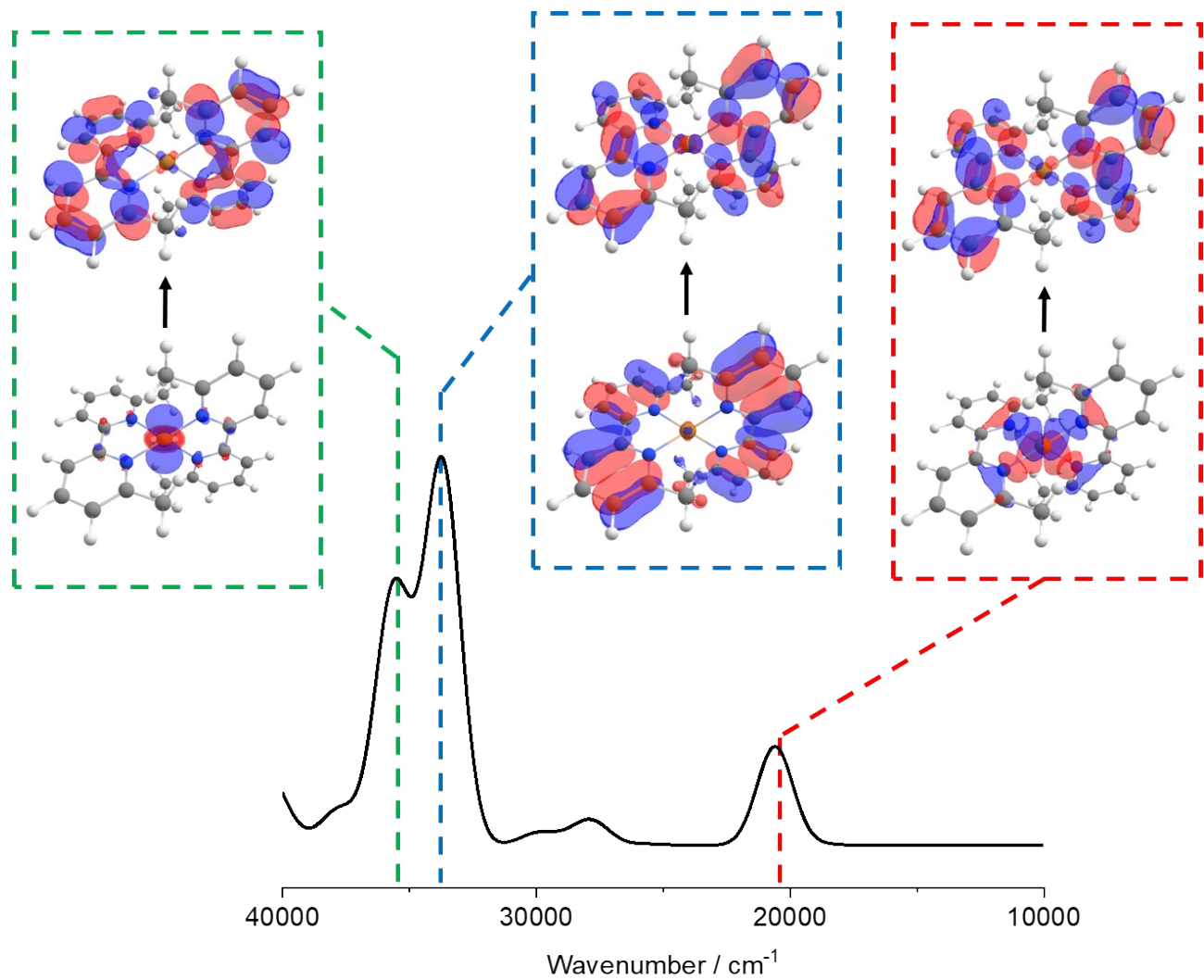


Figure S6. Natural Transition Orbital analysis of the principal contributions to the simulated spectrum of Cu^IBPA.

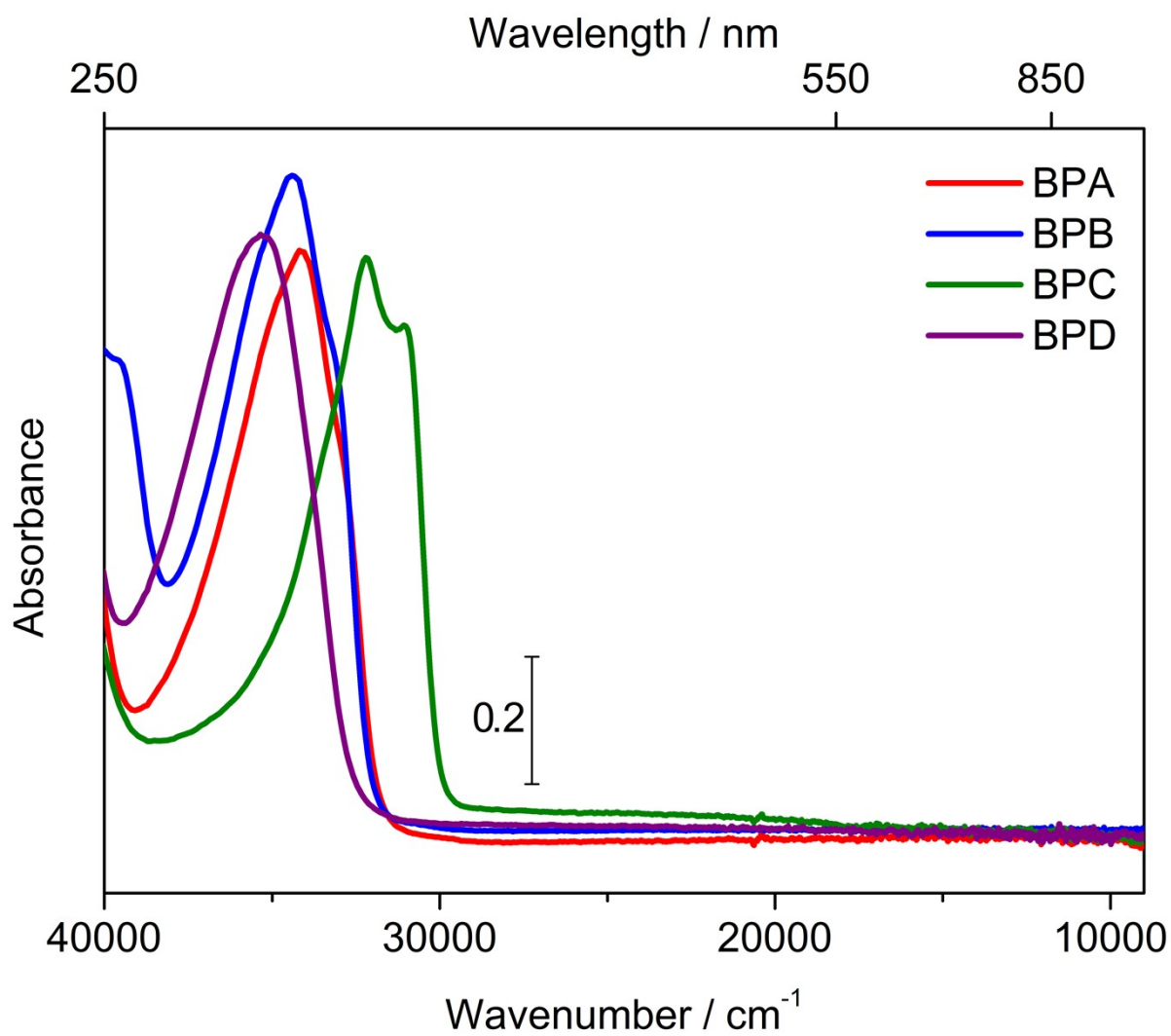


Figure S7. UV-Vis-NIR spectra of the four ligands in their pristine form (1 mM).

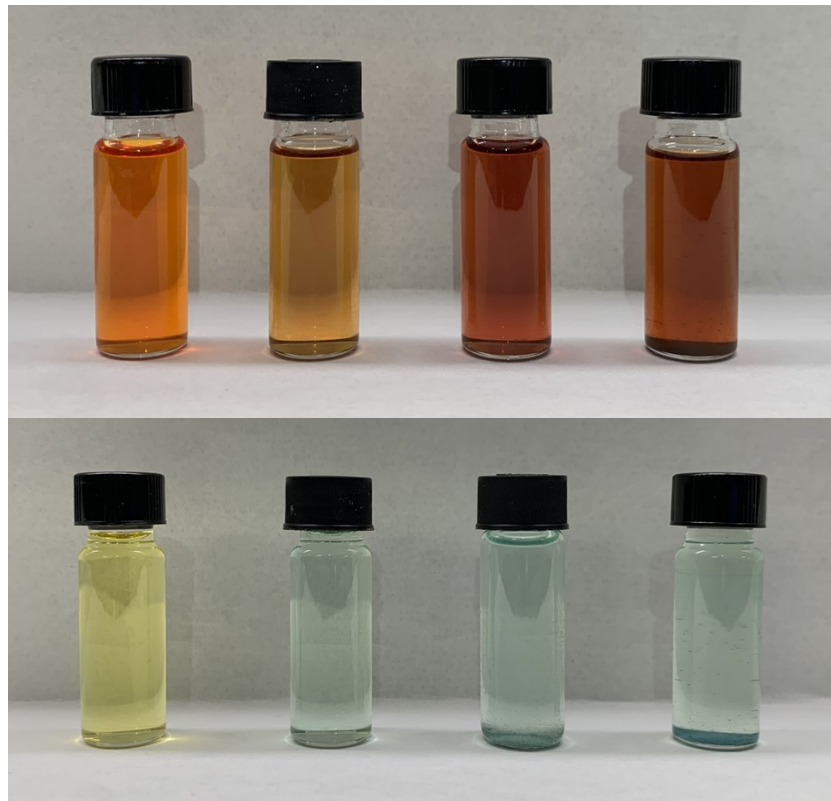


Figure S8. Different samples (CuBPA, CuBPB, CuPBC and CuBPD from right to left) dissolved in DCM before (top) and after (bottom) the addition of tBuOOH. Sample concentration: 1 mM. Final concentration of tBuOOH 20 mM.

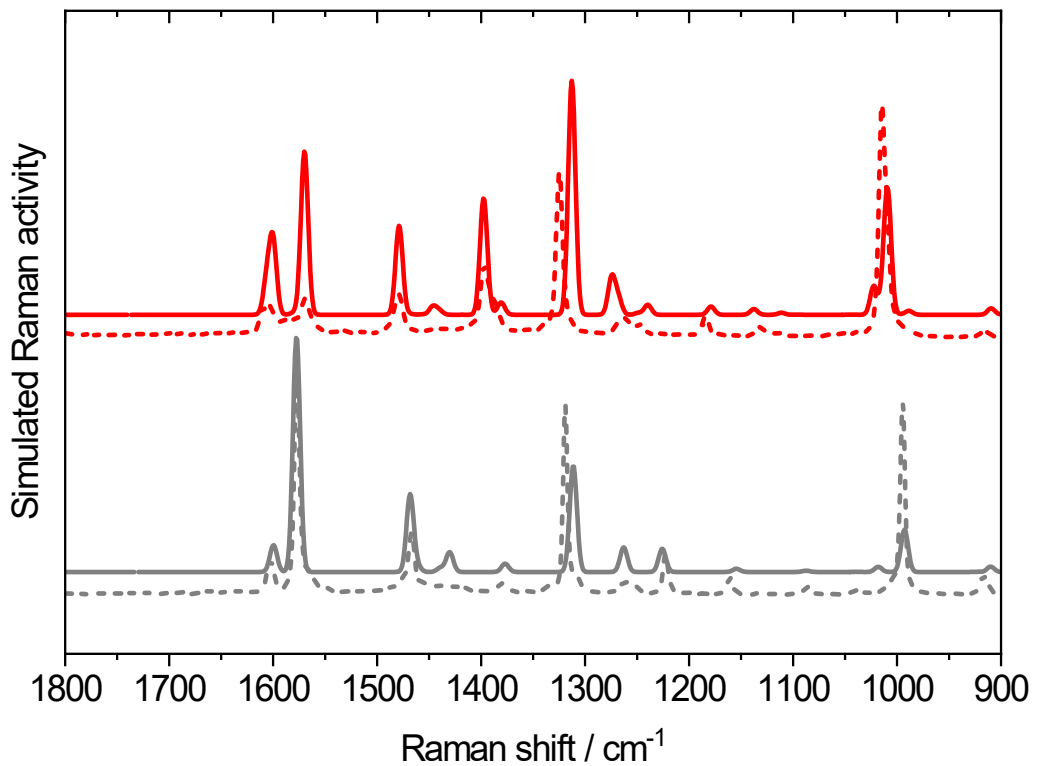


Figure S9. Computed (solid lines) Raman spectra vs experimental ones (dashed lines) for Cu-BPA (ligand, in grey, and complex, in red). Experimental Raman has been collected with a 785 nm excitation wavelength. Simulated spectra have been convoluted with Gaussian functions (FWMH set to 5 cm^{-1}). Computed vibrational frequencies have been scaled by a multiplicative factor (0.978).

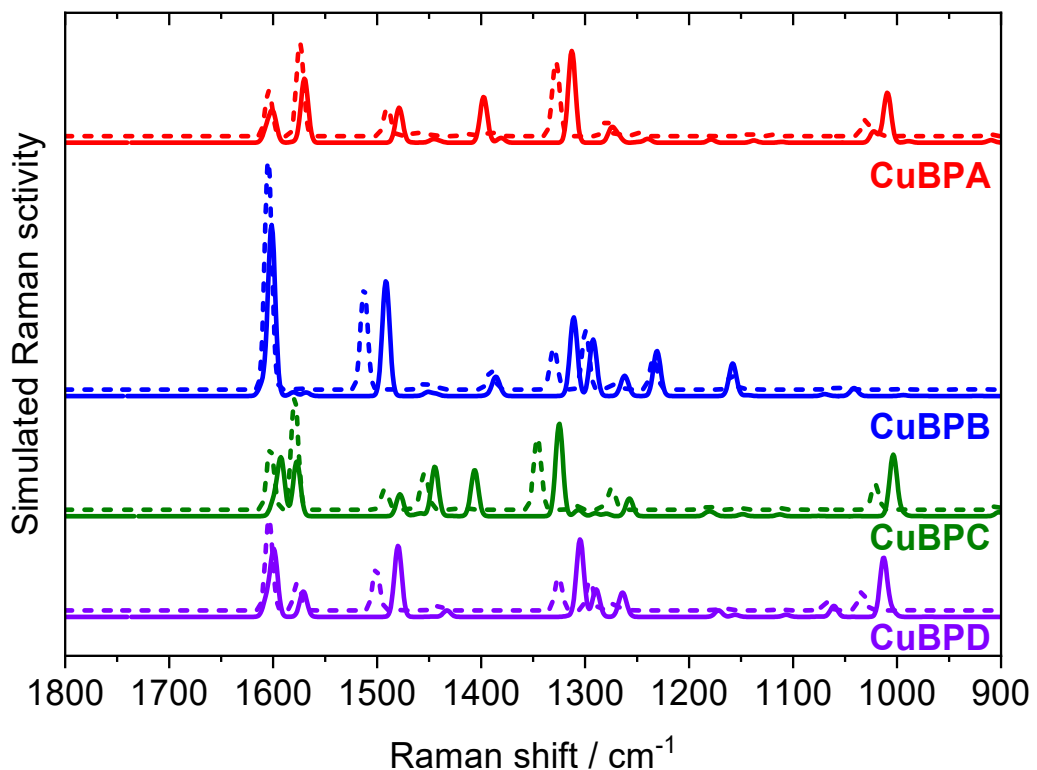


Figure S10. Computed Raman spectra for all Cu complexes in Cu^{I} (solid lines) and Cu^{II} (dashed lines) forms. Simulated spectra have been convoluted with Gaussian functions (FWMH set to 5 cm^{-1}). Computed vibrational frequencies have been scaled by a multiplicative factor (0.978).

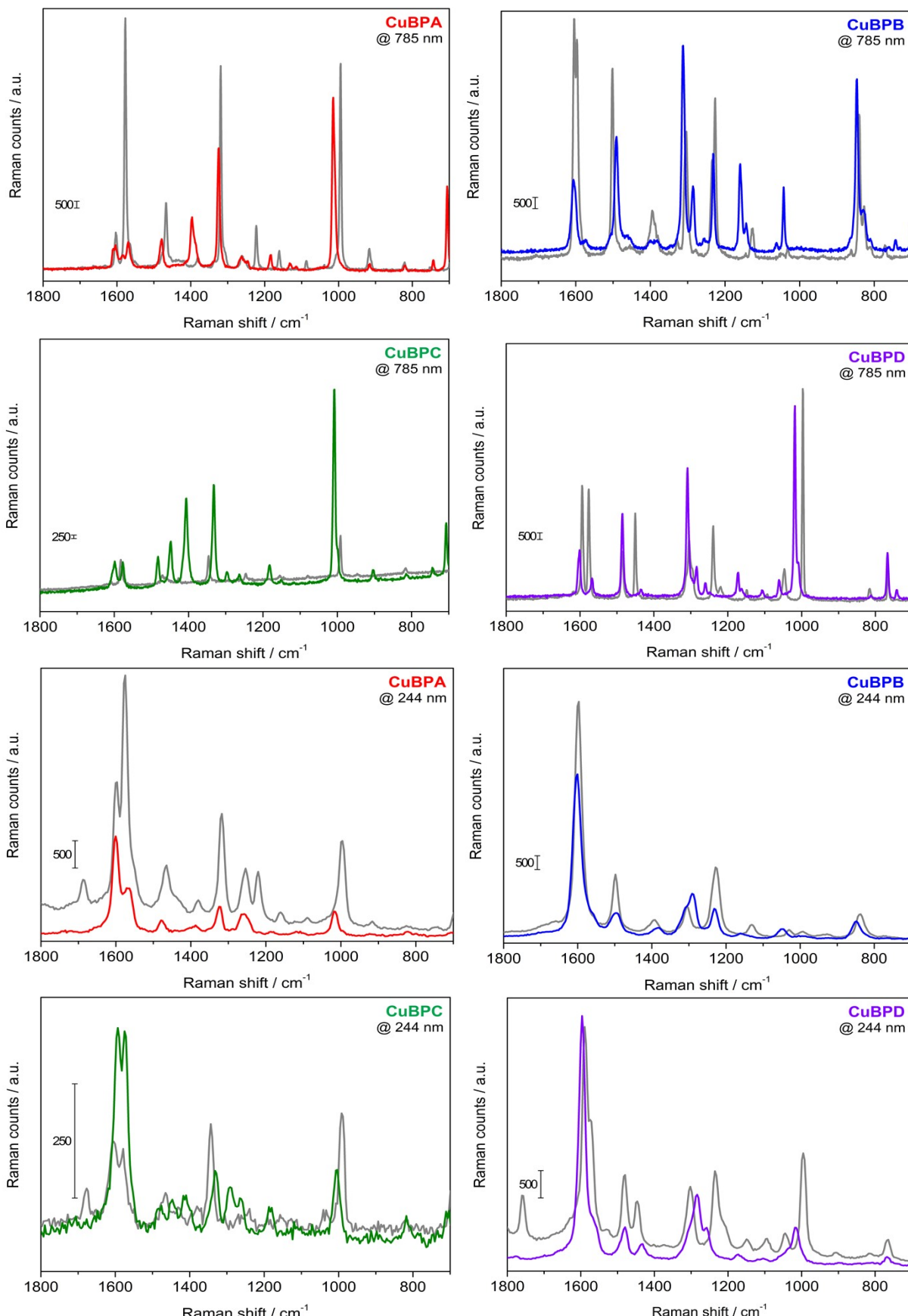


Figure S11. Raman spectra obtained on solids powders of Cu containing complexes (red/CuBPA, blue/CuBPB, green/CuBPC, violet/CuBPD) by adopting exciting laser line falling respectively at $\lambda=785$ nm (red panel) and $\lambda=244$ nm (purple panel). Gray solid lines show Raman spectra obtained from the respective parent ligands.

Assignment of vibrational modes (Raman) by means of computational approach.

In order to produce a starting reference data-set for the assignment of vibrational features characterizing the above described complexes, Raman spectra were initially recorded on solid powders of pristine complexes and their parent ligand: in this case, an exciting laser line with $\lambda=785$ nm ($\tilde{\nu}=12739\text{ cm}^{-1}$) has been adopted (see Experimental section for further details). The reason for this choice is that the associated energy, far from that one characteristic for the electronic transitions (*vide infra*) of the investigated complexes (and ligands), avoids any possible Resonance effects, easing the comparison between experimental and computed conventional Raman spectra even in terms of peak intensity. The full set of the obtained Raman spectra is reported in Figure S12. Hereafter the results obtained on the representative CuBPA complex and the parent ligand (BPA) will be discussed.

On the basis of the DFT results, the Raman spectrum of both Cu-BPA and BPA ligand can be divided into two main regions: a high-frequency one ($1300\text{-}1700\text{ cm}^{-1}$), dominated by the vibrational modes from the aromatic rings (C=C stretching modes) and methyl groups (C-H bending modes), and a low frequency one ($<1300\text{ cm}^{-1}$). The principal feature of the latter region can be assigned to aromatic ring breathing modes with significant involvement of the Cu-N bonds, being, in turn, extremely sensitive to the effective charge of the Cu cation and to the eventual presence of additional ligands in the first coordination sphere. As it can be seen from the grey dotted line in Figure 1, the Raman spectrum of BPA is dominated by three major bands located respectively at 994 cm^{-1} (v_1), 1319 cm^{-1} (v_2) and 1577 cm^{-1} (v_3). Other minor features are present respectively at 1222 cm^{-1} (v_4), 1469 cm^{-1} (v_5), and 1603 cm^{-1} (v_6).

Some not negligible differences (*e.g.* the different v_1^M/v_3^M intensity ratio) fairly depend on the adopted experimental conditions and set-up too (*i.e.* the energy of the source and type of detector). Despite this, the computed (and scaled) Raman spectrum (solid grey line in Figure 1) obtained on the *trans*-BPA conformer as isolated molecule reproduced quite well the experimental one, suggesting the same conformer is present in the solid form too. This is further confirmed from the comparison of Raman spectra of BPA and BPD, where the presence of the *trans* conformer is confirmed by X-ray diffraction,^{1,2} and in agreement with calculations from which the *trans*-BPA (*trans*-BPD) resulted to be more stable than the *cis* one ($\Delta G_{\text{BPA}} = -20.9\text{ kJ mol}^{-1}$, $\Delta G_{\text{BPD}} = -15.3\text{ kJ mol}^{-1}$): this is most probably related to the unfavourable alignment that the $\mu_{\text{N-C}}$ dipoles undergoes in the *trans*->*cis* transition (the final computed μ_{cis} and μ_{trans} for BPA being respectively 3.51 and 0.01 Debye). Moreover, the good correspondence between computed and experimental data (solid compound) makes the former a valuable support to precisely assign the experimental vibrational features. In particular, from the analysis of the computed vibrational modes associated with each peak, it can be observed that: a) v_1 strongly involves N atoms and the 2 C atoms forming a 120° angle with N and the centre of mass (CM) of the pyridine ring; in fact, it can be described as the symmetric combination of N-CM and C-CM stretching; b) v_2 can be assigned to the stretching of the C-C moiety connecting the two pyridine rings; c) v_3 can be assigned to the symmetric combination of C-N and C-C (located on the opposite side of pyridine ring) stretching.

Passing to the Raman spectrum obtained on the solid forms of Cu-BPA complex, the structure of which (2 *cis*-BPA ligands chelating, in a slightly distorted tetrahedral fashion, a Cu⁺ ion) has been well characterized from X-Ray Diffraction,^{3,4} it can be observed that two major features (v_{Cu_1} and v_{Cu_2}) are present, centred

respectively at 1014 cm^{-1} and 1324 cm^{-1} . The region around 1600 cm^{-1} is instead characterized by two weak features v^{Cu}_3 and v^{Cu}_4 located respectively at 1570 cm^{-1} and 1601 cm^{-1} and a very weak one (v^{Cu}_5) centred at 1584 cm^{-1} . Finally, two more minor features (v^{Cu}_6 and v^{Cu}_7), located respectively at 1397 cm^{-1} and 1479 cm^{-1} , are visible. A specific assignation of these modes falls out of the scope of the present work, and it will be tackled in a forthcoming paper specifically dedicated to the Raman spectroscopy's features.

Even in this case, the experimental spectra find a good correspondence in the computed ones, allowing a confident assignment of the observed peaks to defined vibrational modes. Without entering in further details, it is worth noticing here that v^{Cu}_1 (now involving 4 N atoms) and v^{Cu}_2 correspond to vibrational modes described above for v_1 and v_2 respectively for the BPA case, and that they fall at Raman shift higher than those observed for BPA ligand ($\Delta v^{\text{Cu}}_1=+10\text{ cm}^{-1}$ and $\Delta v^{\text{Cu}}_2=+5\text{ cm}^{-1}$). This is quite expected for v_1 , because its associated vibrational mode directly involves N atoms responsible for Cu coordination in the CuBPA complex, as evidenced from X-ray resolved structures too^{4,5}. Furthermore, the comparison between computed v_1 obtained on *trans*-BPA and on *cis*-BPA (*i.e.* Δv_1 due to change in conformation which results to be $+6\text{ cm}^{-1}$) allows to conclude that the observed blue-shift on passing from bare *trans*-BPA to CuBPA could be ascribed to the effect (partly due to electrostatics and partly due to charge-transfer phenomena) of the Cu^+ coordinating species: this makes v^{Cu}_1 a good candidate to be a vibrational probe of the Cu oxidation state and local environment in the complex.

The data discussed above have been obtained for solids powder and using a 785 nm exciting laser line: unfortunately, it has been verified that the chosen experimental set-up was unable to produce enough detailed Raman spectra of complexes at working conditions adopted for UV-Vis-NIR measurements (10^{-3} M in DCM). For this reason, it was decided to exploit the Resonant conditions by adopting an exciting laser line with energy falling in the range where highly favoured electronic transitions are located. Figure S10 shows that the strongest absorption in the UV-Vis occurs in the UV energy range ($40000\text{-}35000\text{ cm}^{-1}$) for 1 mM DCM BPA/CuBPA solutions: for this reason, among the available exciting laser lines in our laboratory, the 244 nm ($\tilde{\nu}=40984\text{ cm}^{-1}$) one was selected. Preliminary test measurements have been performed on solids powders of both BPA and CuBPA model systems (see Figure S11), obtaining the same vibrational features (at least in terms of Raman shifts) as discussed for the 785 nm case. However, for the 244 nm Raman spectra, a complete inversion of relative intensity between the peaks centred around 1000 cm^{-1} (v_1 and v^{Cu}_1) and those nearby 1600 cm^{-1} (v_6 and v^{Cu}_{3-5}) can be observed, the latter being now more intense than the former. Despite this, the observed and previously discussed Δv^{Cu}_1 can be still clearly distinguished. On passing to 1 mM DCM solutions of BPA/CuBPA systems, the corresponding Raman spectra obtained with the 244 nm laser line are shown in Figure S4. When comparing these with spectra obtained on BPA/CuBPA solid powders, it can be noticed that signals ascribable to Raman fingerprints of BPA/CuBPA molecules are still clearly observable even at this low concentration. Unfortunately, Raman spectra at Raman shift lower than 900 cm^{-1} are overshadowed by a very intense peak (DCM) and from signals coming from cuvette walls containing the investigated solutions, jeopardizing the possibility to individuate further Raman fingerprints characterizing BPA/CuBPA molecules. For this reason, in the following, the $1800\text{-}900\text{ cm}^{-1}$ interval of the whole spectrum will be presented.

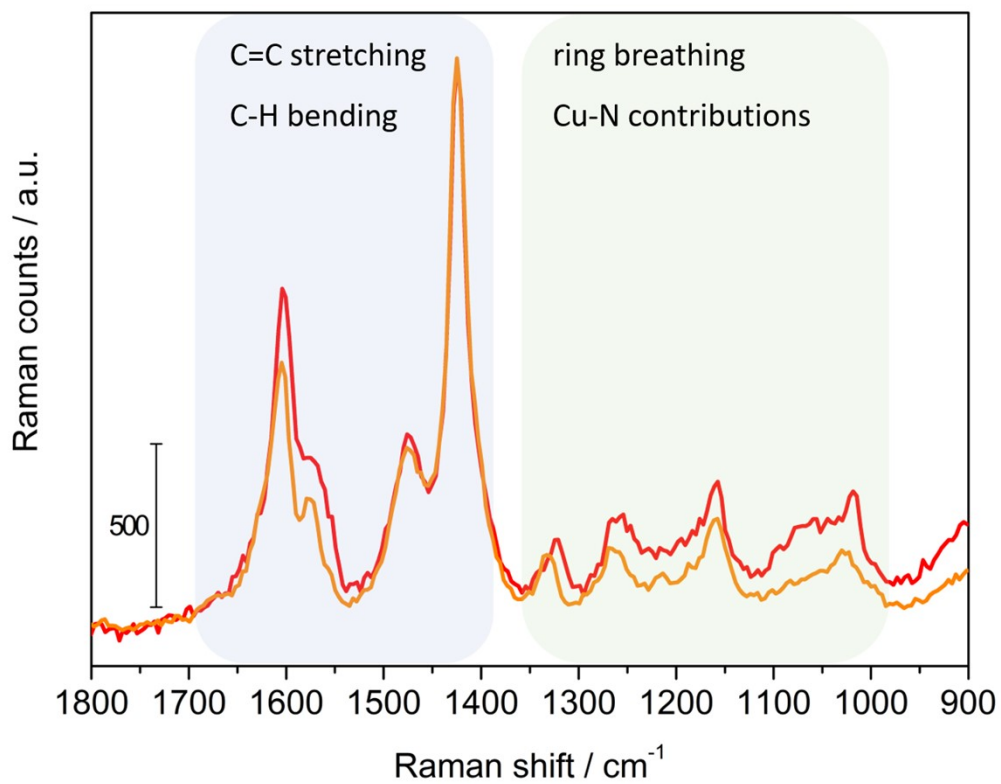


Figure S12. Raman spectra of pristine CuBPA (red line) and after oxidation with tBuOOH (orange line). Sample concentration: 1 mM in DCM. Final concentration of tBuOOH 20 mM.

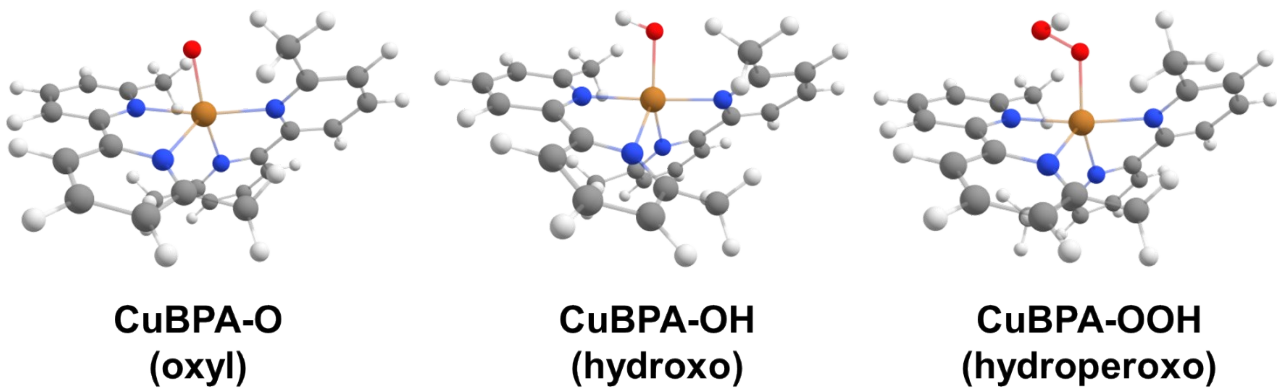
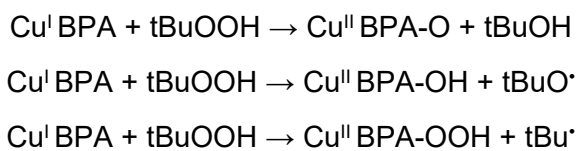
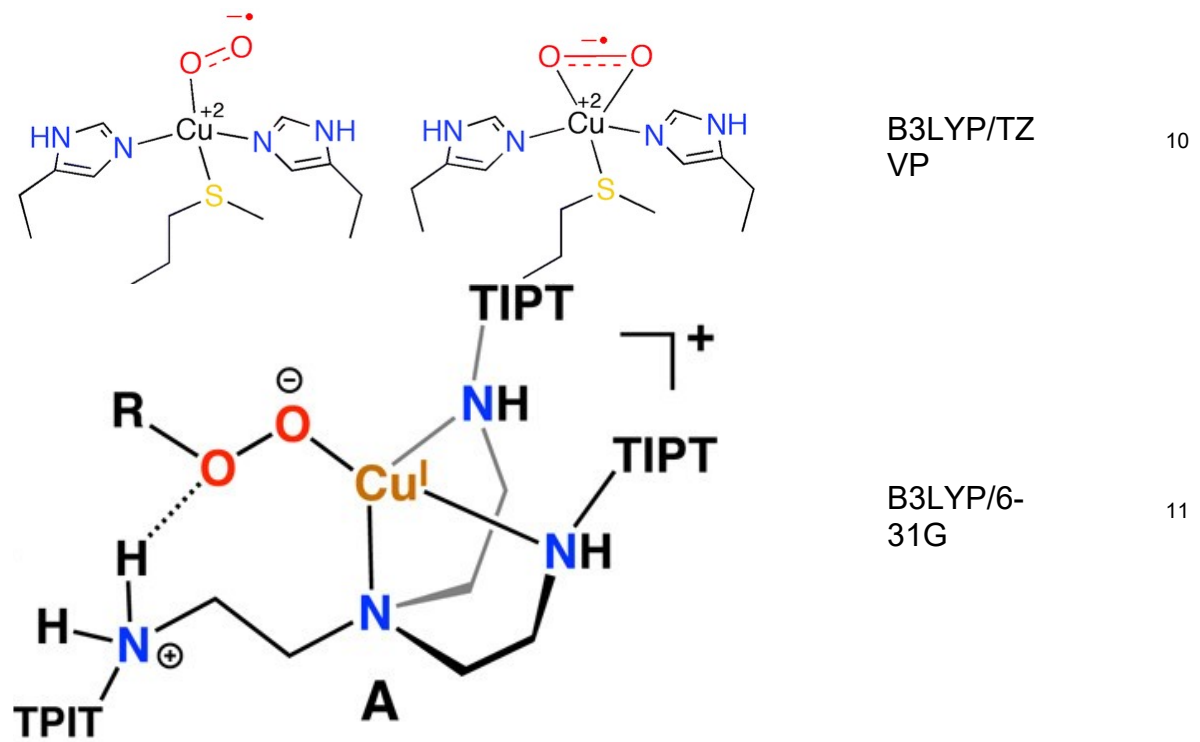


Figure S13. Optimized DFT structures of CuBPA bearing a Cu-O_x specie: CuBPA-O (oxyl), CuBPA-OH (hydroxo) and CuBPA-OOH (hydroperoxo).

Table S2. Literature examples of (TD-)DFT investigations involving Cu-complexes with oxygenated species.

Reference	Structure	Method	Reference
		PBE0/TZV P	6
		BP86/TZV P	7
		B3LYP/6-311G*	8
		B3LYP/6-311G*	9



Scheme S1. Reactions considered in the calculation of formation energies for CuBPA-O, CuBPA-OH and CuBPA-OOH.

Table S3. Average Cu-N distance ($\langle d_{\text{Cu-N}} \rangle$, in Å), Cu-O distance ($d_{\text{Cu-O}}$, in Å), angle among the planes defined by the aromatic systems of each bpy ligand (τ , in °), Mulliken spin densities on Cu (ρ_{Cu}) and O bound to it (ρ_{O}) for the CuBPA bearing a Cu-O_x specie (oxyl, hydroxo and hydroperoxo)

Model	$\langle d_{\text{Cu-N}} \rangle$	$d_{\text{Cu-O}}$	τ	ρ_{Cu}	ρ_{O}
CuBPA-O	2.13 ± 0.09	1.881	72.6	0.546	1.188
CuBPA-OH	2.13 ± 0.11	1.921	68.9	0.598	0.185
CuBPA-OOH	2.12 ± 0.09	1.953	69.2	0.527	0.246

The introduction of oxygenated species in the ligand sphere of CuBPA causes a distortion of the complex (as already observed in the case of the purely electronic oxidation), as well as an elongation and an heterogenization of the Cu-N bond distances. In overall, the coordination environment around Cu in CuBPA bearing a Cu-O_x specie can be described as a distorted trigonal bipyramidal.

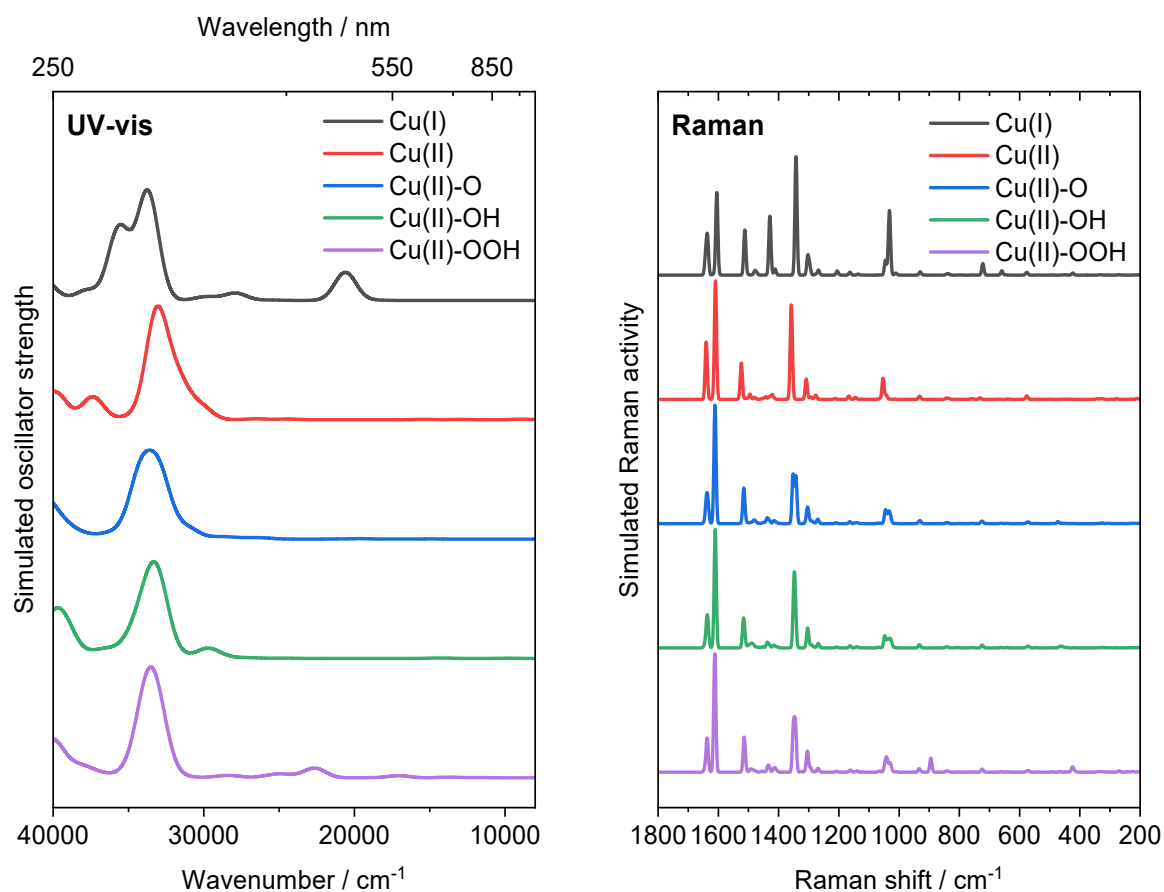


Figure S14. Computed UV-Vis (left) and Raman (right) spectra for Cu-BPA, also bearing Cu-O_x species (namely oxyl, hydroxo and hydroperoxo in blue, green and purple, respectively). Simulated spectra have been convoluted with Gaussian functions (FWMH set to 1000 cm⁻¹ for UV-Vis, to 5 cm⁻¹ for Raman). Computed vibrational frequencies have been scaled by a multiplicative factor (0.978).

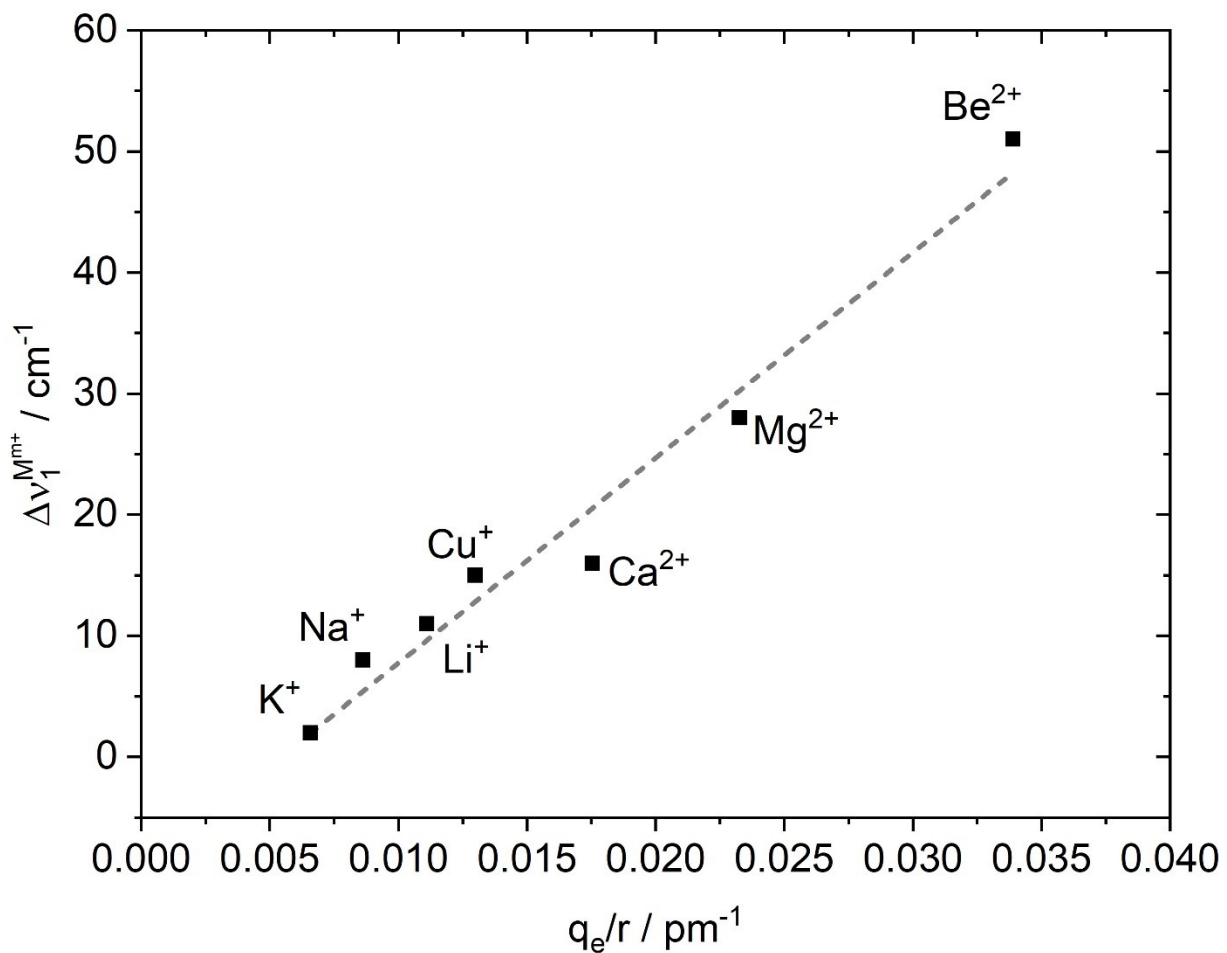


Figure S15. Correlation of $\Delta\nu_1$ with the elementary charge/ionic radius ratio for $M^{m+}(cis\text{-BPA})_2$ (where $M^{m+} = \text{Li}^+, \text{Na}^+, \text{K}^+, \text{Be}^{2+}, \text{Mg}^{2+}$ or Ca^{2+}) complexes, calculated with respect to the free trans-BPA ligand.

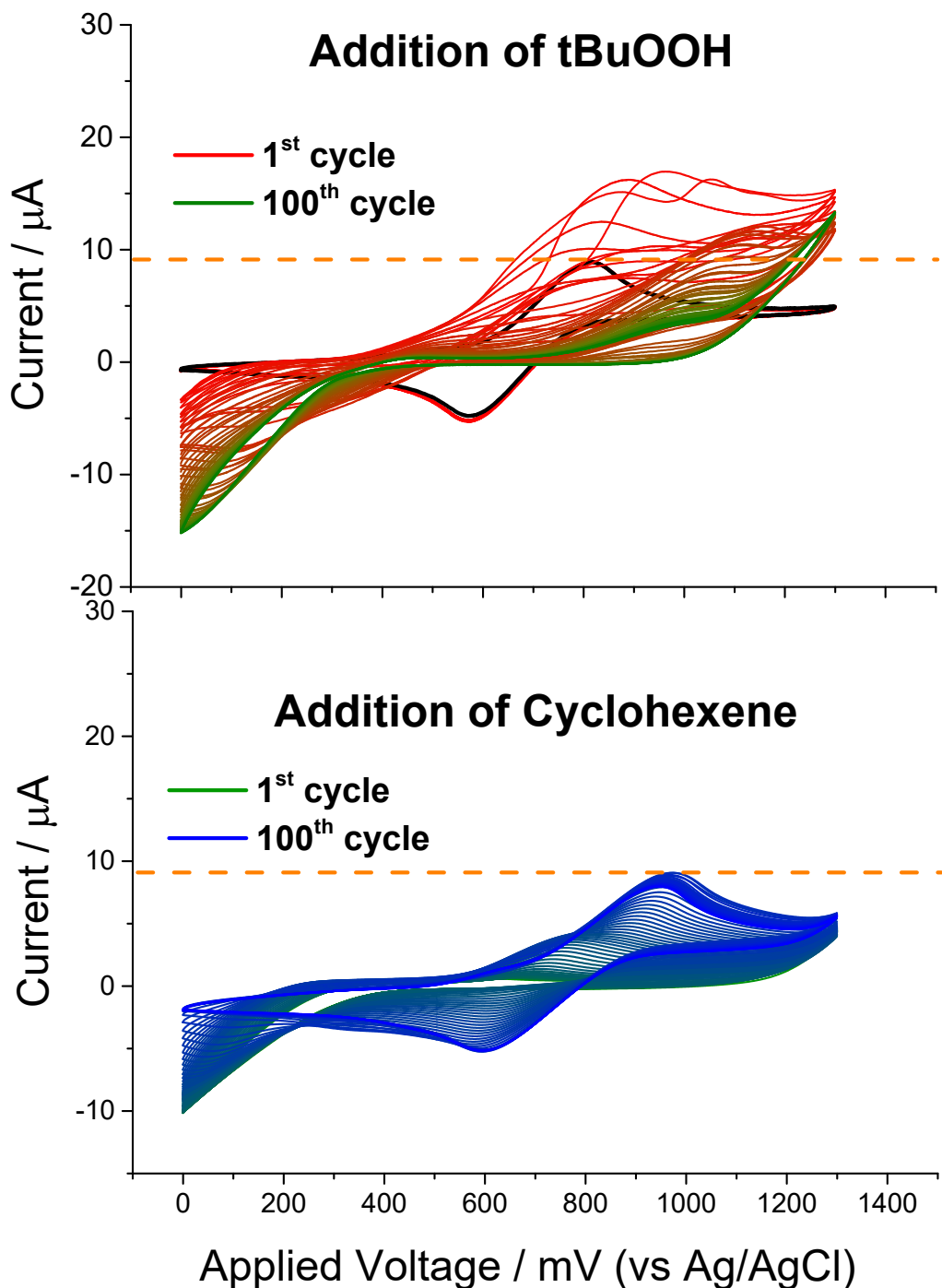


Figure S16. Evolution of CV voltammogram of oxidized (tBuOOH) CuBPA after the addition of cyclohexene.

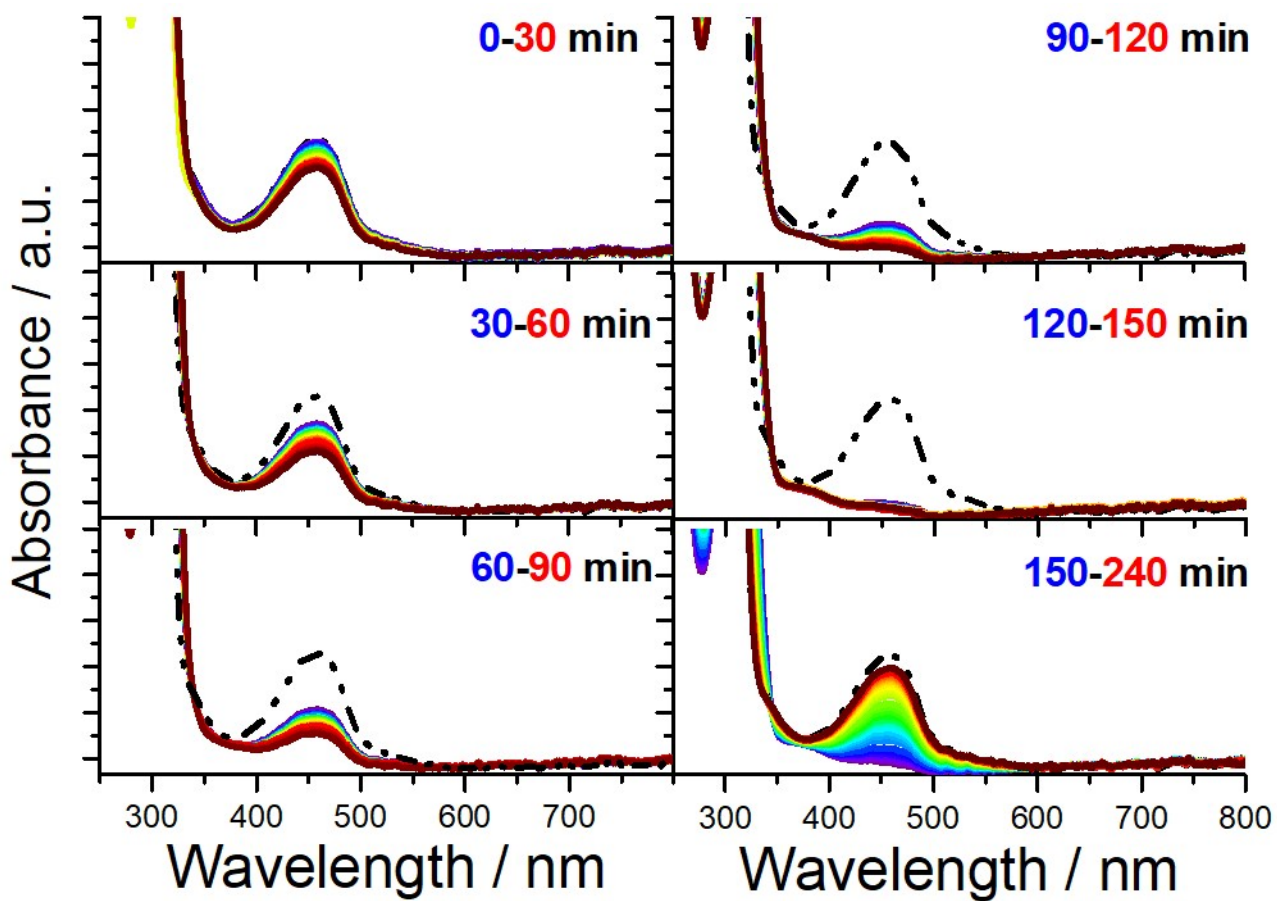


Figure S17. Evolution of the UV-Vis spectrum of CuBPA (1 mM) after the addition of tBuOOH (Final concentration of 20 mM, added at $t=0$ minutes) and the addition of cyclohexene (equimolar respect to tBuOOH, $t = 150$ minutes)

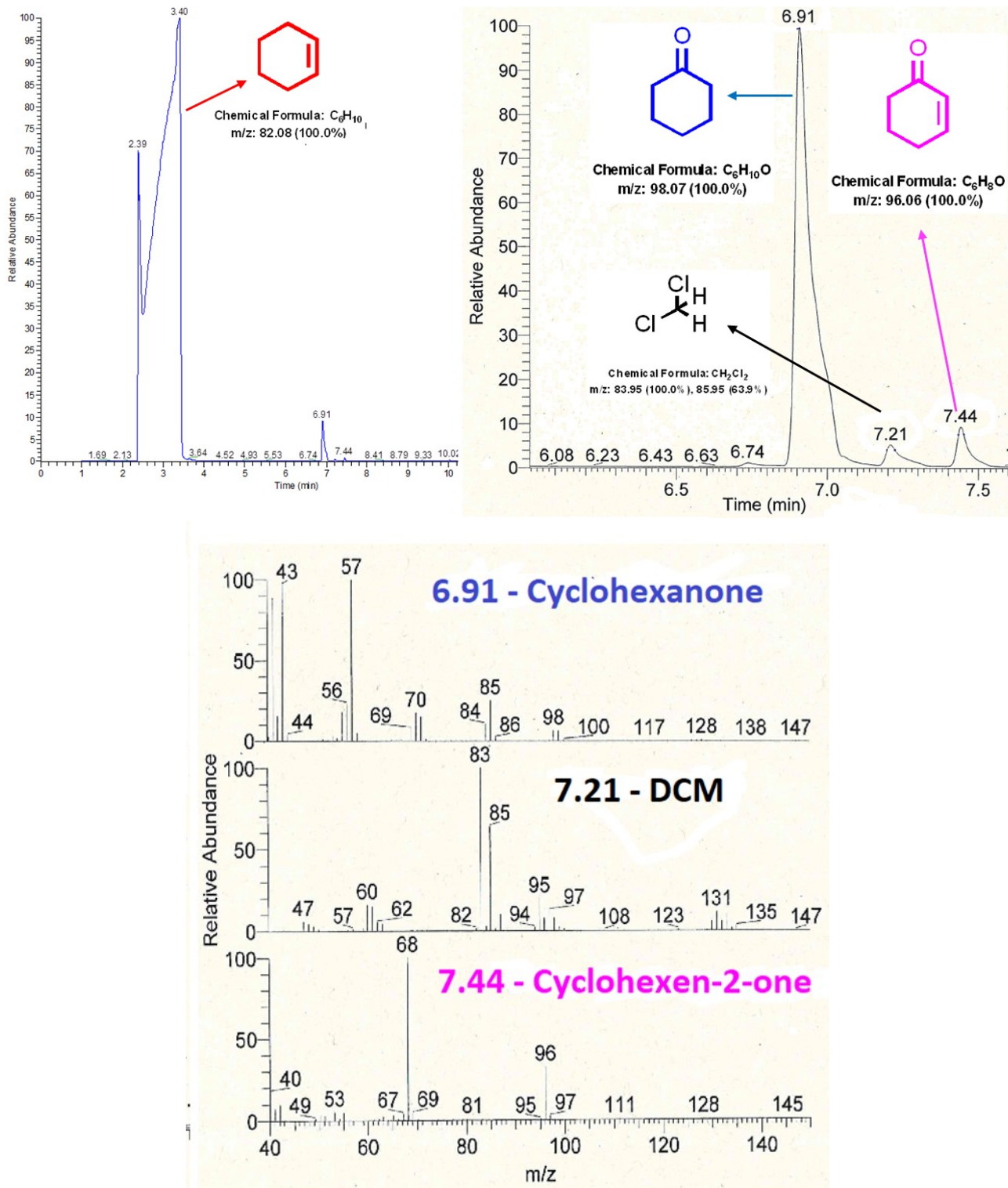


Figure S18. GC-MS spectra of CuBPA (8 mM) after the addition of tBuOOH (0.160 M) and then the addition of cyclohexene (0.160 M). Top left: Full chromatogram; Top right: zoom of the chromatogram in the range 6-7.5 min; bottom, MS of selected peaks.

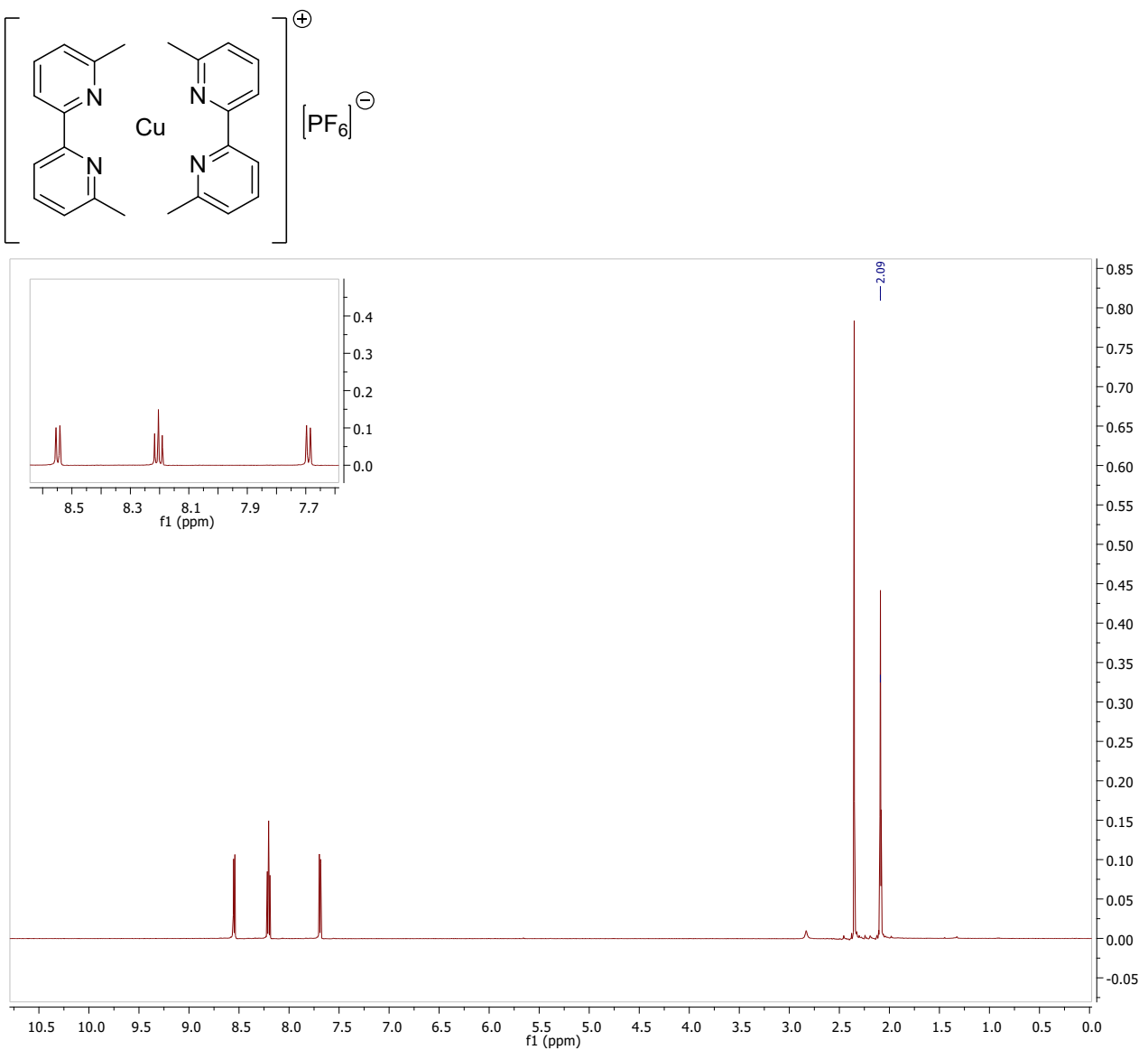


Figure S19. CuBPA NMR spectrum acquired at -40°C

^1H NMR (600 MHz, $(\text{CD}_3)_2\text{CO}$) δ 8.55 (d, $J = 8.0$ Hz, 1H), 8.20 (t, $J = 7.9$ Hz, 1H), 7.69 (d, $J = 7.7$ Hz, 1H), 2.35 (s, 3H), 2.09 (solvent residual peak).

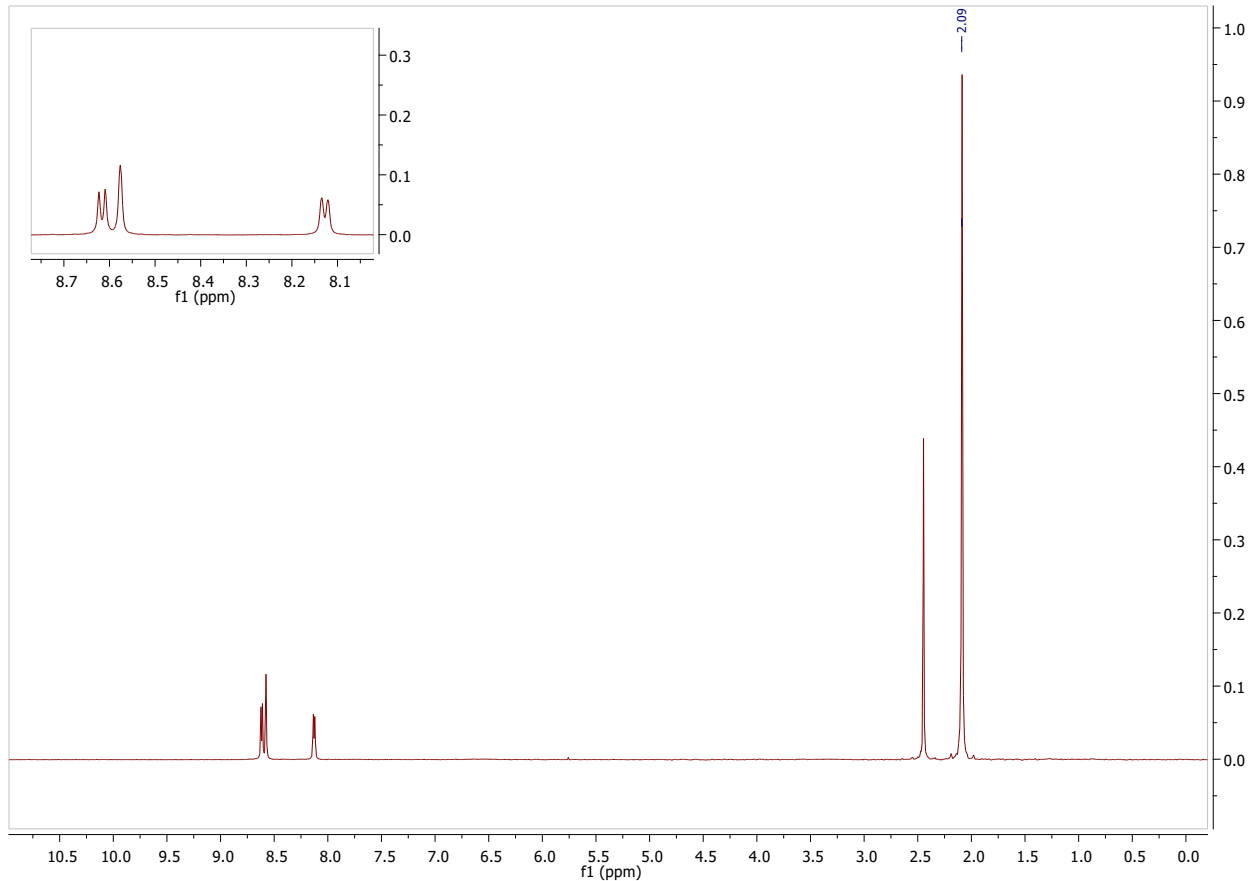
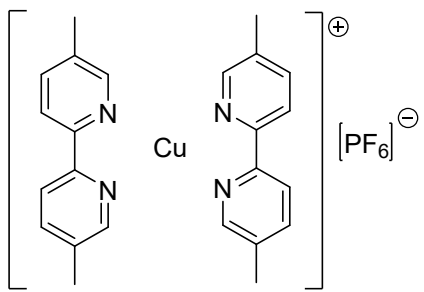


Figure S20. CuBPB NMR spectrum acquired at -40°C

^1H NMR (600 MHz, $(\text{CD}_3)_2\text{CO}$) δ 8.62 (d, $J = 8.3$ Hz, 1H), 8.58 (s, 1H), 8.13 (d, $J = 8.1$ Hz, 1H), 2.45 (s, 3H), 2.09 (solvent residual peak).

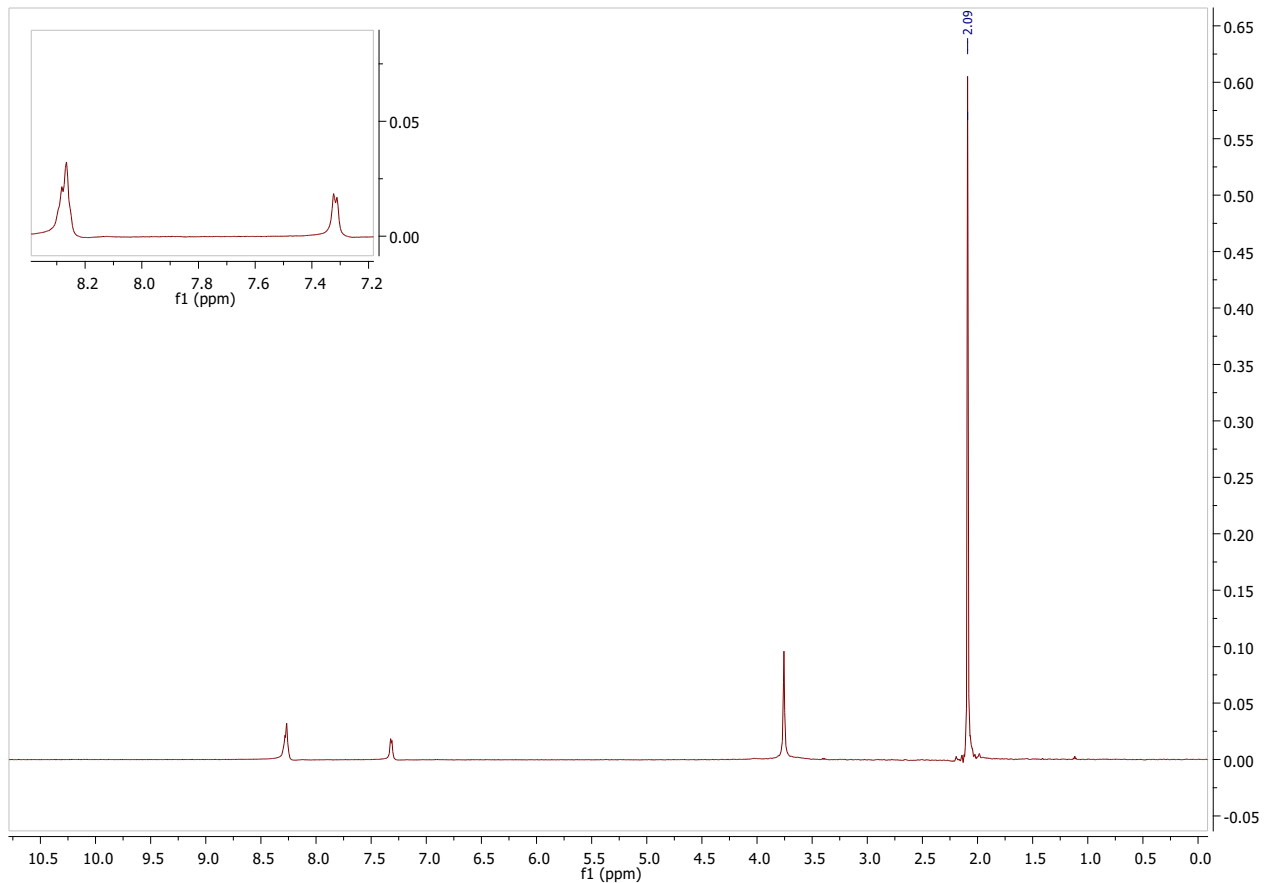
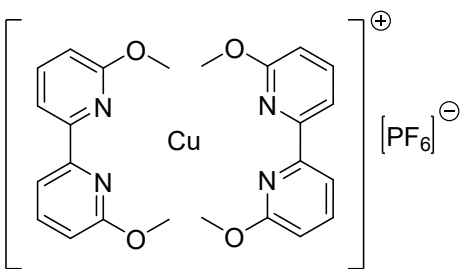


Figura S21. CuBPC NMR spectrum acquired at -40°C

¹H NMR (600 MHz, (CD₃)₂CO) δ 8.27 (m, 2H), 7.32 (d, J = 7.0 Hz, 1H), 3.76 (s, 3H), 2.09 (solvent residual peak).

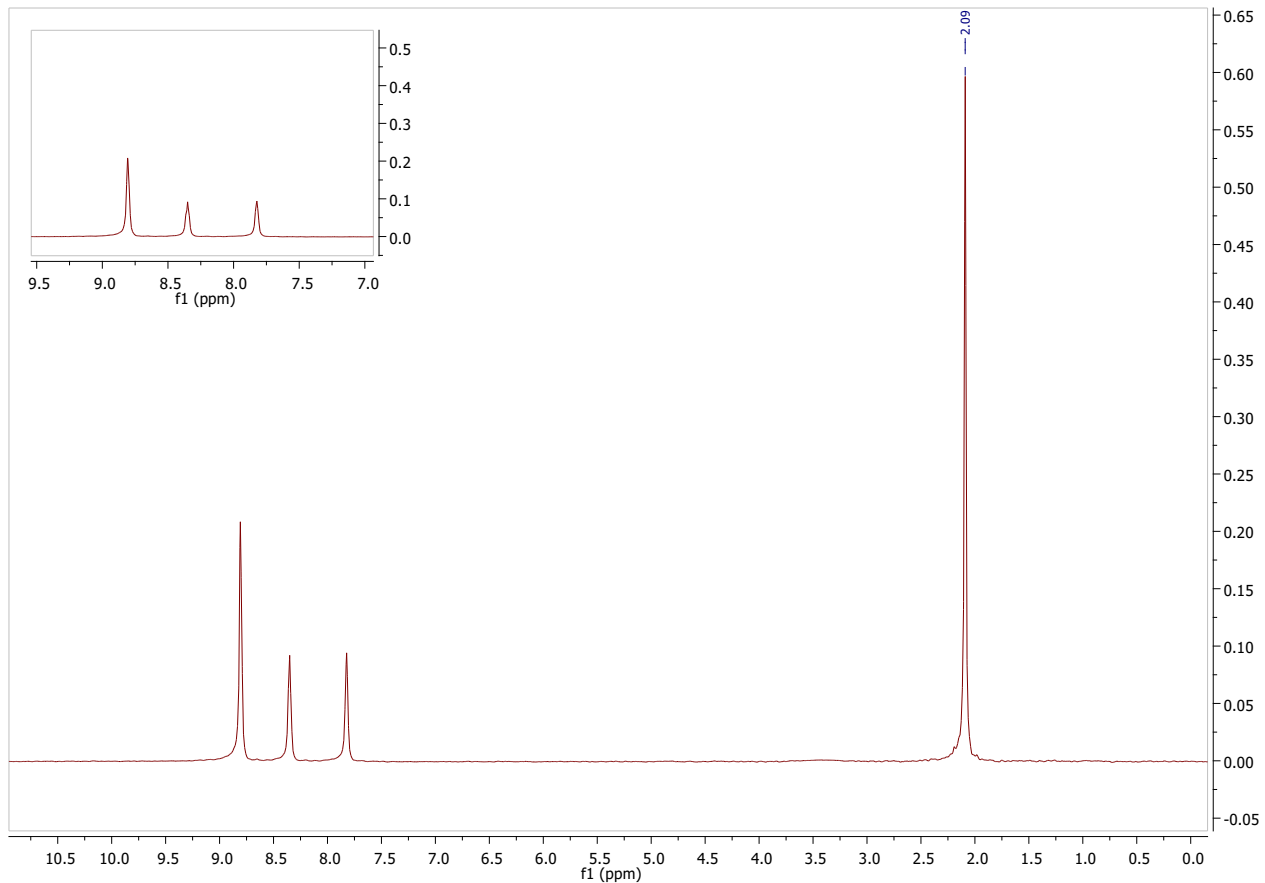
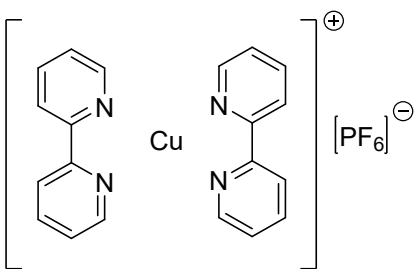
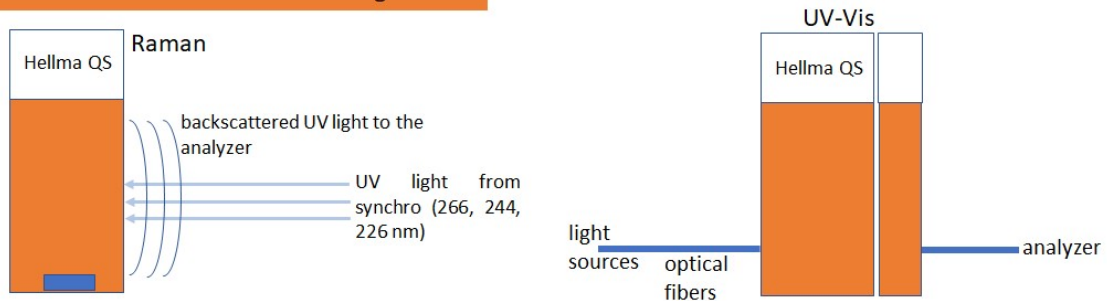


Figure S22. CuBPD NMR spectrum acquired at -40°C

^1H NMR (600 MHz, $(\text{CD}_3)_2\text{CO}$) δ 8.81 (s, 1H), 8.35 (s, 1H), 7.82 (s, 1H), 2.09 (solvent residual peak).

The synthesized copper complexes have been characterized by means of NMR spectroscopy to prove the success of the used synthetic pathway. The spectra have been recorded using acetone-d6 as the solvent, as all the complexes show a very good solubility and a relatively stability in the latter. The room temperature acquired spectra results in extremely broad and uninformative signals, except for CuBPA. This is probably due to the presence in solution of dynamic coordination balances, that in the cases of CuBPB, CuBPC and CuBPD occur in shorter or comparable times respect to the NMR time scale. As a matter of fact, the reported spectra (Figure S19-S22) have been acquired at -40°C to obtain spectra with improved resolution, that means sharper peaks and the possibility of appreciating multiplicity for almost all the samples. Actually, the -40°C recorded spectra of CuBPD, shows quite broad signals and a consequent lack of multiplicity. This is ascribable to the presence of traces of Cu(II) that interfere with the acquisition due to the paramagnetic nature of the Cu(II) species. In fact, the CuBPD complex is prone to the oxidation to Cu(II) state very quickly in acetone solution and after few minutes a blue/green powder starts precipitating in the tube. Nevertheless, the couple acetone/low temperature ensure a good quality of the NMR spectra, that confirms the formation of the desired complexes.

In situ Raman and UV-Vis measurements configuration



Simultaneous measurements configuration

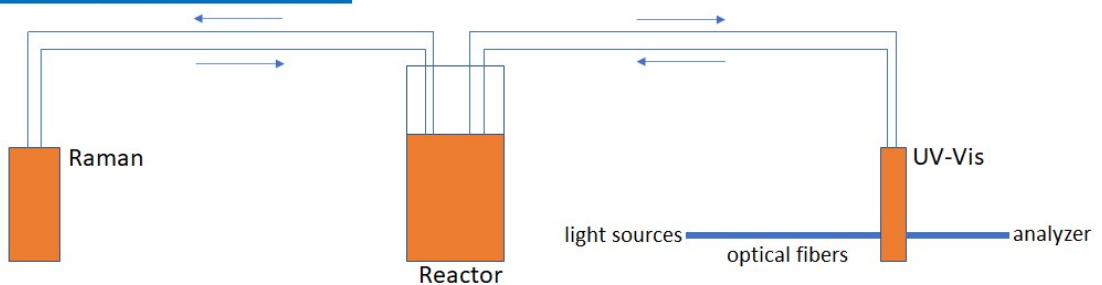


Figure S23. Custom-made experimental set-up employed to perform single (top) and simultaneous (bottom) spectroscopic measurements.

Optimized DFT structures

Structures for all DFT optimized models provided in this work are reported hereafter in .xyz format.

- **CuI-BPA.xyz:**

53
CuI-BPA
H 2.8655699042 -0.529677438 -3.9851448543
C 3.5928202313 -0.0851246168 -0.721171209
H 4.399388071 0.1900326238 -0.0566170303
C 3.7851114212 -0.1333758041 -2.0933288557
H 4.7492345543 0.106853225 -2.5205744114
C 2.7290796306 -0.4923341475 -2.9158159435
C 1.5003276993 -0.7956009669 -2.3378301713
N -0.8178350226 -1.403987116 -2.4272465961
C -1.9498415162 -1.7629559976 -3.0491593209
C -3.1573792813 -1.9764952215 -2.1910174447
H -4.0271149119 -2.2392230797 -2.7898075061
H -2.9721713367 -2.7738875487 -1.468804319
H -3.378731496 -1.0735397167 -1.6191948415
N 1.3262006275 -0.7397346346 -1.0042454828
C 2.3406177106 -0.3948149646 -0.1985999508
C 2.0584986017 -0.3593495145 1.2708570715
H 1.697238166 -1.3320046097 1.609592164
H 1.2721225912 0.3660939532 1.4878164016
H 2.9481546938 -0.0941160187 1.8384649265
C -1.9833405027 -1.926962676 -4.4308180322
H -2.9050282434 -2.2158749976 -4.9155001947
C -0.8268323016 -1.7174832851 -5.1661598759
H -0.829986831 -1.8428385897 -6.2404308831
C 0.3369633327 -1.3456477371 -4.512051674
C 0.31091508 -1.1923792519 -3.129409128
H 1.2438816004 -1.1835785935 -5.0730518827
H -3.0583945554 -2.5031460318 3.7509703904
C -1.2542347868 -4.7294736643 1.9709376454
H -0.9706066077 -5.7719715789 1.9454696466
C -2.0752255218 -4.2386927429 2.9745456519
H -2.4470968749 -4.8957682693 3.7489781057
C -2.4172249294 -2.8957232822 2.9774892664
C -1.9241652221 -2.074652704 1.9682296925
N -1.7183765821 0.0205136877 0.8193449753
C -1.9391565586 1.3316395097 0.6482369501
C -1.3343279331 1.9693731172 -0.5632217719
H -1.5910532289 3.0249861289 -0.6247752168
H -0.2473345688 1.8712942507 -0.5396918254
H -1.6803662076 1.4657610452 -1.4676217593
N -1.1320025577 -2.5655408857 0.996943553
C -0.7936362285 -3.8626242691 0.9843166982
C 0.0913069614 -4.322409589 -0.1317593984
H 1.0201476762 -3.749237222 -0.1378027402

H -0.3945201728 -4.1524606571 -1.0944726106
 H 0.3280239847 -5.3804216259 -0.0390717469
 C -2.6973634001 2.0529042709 1.5657884351
 H -2.8658745356 3.109151461 1.4113822761
 C -3.2252679695 1.4010001745 2.6696264303
 H -3.814443139 1.9432797109 3.396666738
 C -2.9910300888 0.045159998 2.8350633343
 C -2.2291888043 -0.6260131608 1.8837512102
 H -3.3933467494 -0.4720591227 3.6918678941
 Cu -0.5854534311 -1.1722318637 -0.4037721347

- *Cull-BPA.xyz:*

53

Cull-BPA

H -4.8383904566 -0.7846942387 0.6794047584
 C -2.5006459783 -2.7948520583 2.0487328457
 H -2.3860362671 -3.6492275618 2.6991424451
 C -3.7556239182 -2.3094797451 1.7263235743
 H -4.6434557743 -2.7867616398 2.117106794
 C -3.8679048946 -1.1918072559 0.9131538972
 C -2.7126683966 -0.6040943 0.4231601418
 N -1.4965181018 1.1130871396 -0.7193741416
 C -1.3662465777 2.1709495914 -1.5370547807
 C 0.0083604559 2.6383955518 -1.8973706054
 H -0.0453484135 3.4379755353 -2.6316288874
 H 0.5453153777 3.014076007 -1.0270967091
 H 0.5927288051 1.8211588878 -2.3216606899
 N -1.4966066236 -1.113004701 0.7193379503
 C -1.3664230989 -2.1708668542 1.5370357293
 C 0.0081427329 -2.6383779127 1.8974249771
 H 0.5925305029 -1.8211674587 2.321739181
 H 0.5451230467 -3.0140921774 1.0271824514
 H -0.0456431026 -3.437948644 2.6316876105
 C -2.5004160553 2.7950085251 -2.0487818038
 H -2.3857348338 3.6493878117 -2.6991738197
 C -3.7554330611 2.3097069428 -1.7264179681
 H -4.6432244337 2.7870477535 -2.1172212174
 C -3.8678058095 1.1920354353 -0.9132587788
 C -2.7126191904 0.6042500248 -0.4232342072
 H -4.8383229567 0.7849809917 -0.6795387906
 H 4.8383830284 0.7846837446 0.6794473234
 C 2.5006218517 2.7948570404 2.048726276
 H 2.3860042602 3.6492442969 2.6991190402
 C 3.7556035988 2.3094773881 1.7263418647
 H 4.6434308366 2.7867641868 2.1171295875
 C 3.8678945646 1.1917975365 0.9131830473
 C 2.712664026 0.604081037 0.4231793645
 N 1.4965251518 -1.1130980443 -0.7193723299
 C 1.3662639271 -2.1709495454 -1.5370704372
 C -0.0083360763 -2.6383788153 -1.897435874

H 0.0453895704 -3.4379429726 -2.6317101617
 H -0.5453185165 -3.0140757644 -1.0271870341
 H -0.5926873143 -1.8211302224 -2.3217264074
 N 1.4965995457 1.1129937222 0.7193398609
 C 1.3664057196 2.1708667689 1.5370202517
 C -0.0081671476 2.6383944104 1.8973599923
 H -0.5925719215 1.8211958358 2.321673802
 H -0.5451200568 3.0140921194 1.0270924575
 H 0.0456018905 3.4379809798 2.6316066122
 C 2.5004401471 -2.795003395 -2.0487885735
 H 2.3857668137 -3.6493708686 -2.6991975043
 C 3.7554533523 -2.3097092145 -1.7263997932
 H 4.6432493388 -2.7870451209 -2.1171985496
 C 3.8678161184 -1.1920451339 -0.9132296579
 C 2.712623542 -0.6042632647 -0.4232150209
 H 4.8383303684 -0.7849915148 -0.6794961809
 Cu -0.0000000073 -0.0000074156 0.0000131746

- *Cull-BPA-O.xyz:*

54

Cull-BPA-O

H -4.8383904566 -0.7846942387 0.6794047584
 C -2.5006459783 -2.7948520583 2.0487328457
 H -2.3860362671 -3.6492275618 2.6991424451
 C -3.7556239182 -2.3094797451 1.7263235743
 H -4.6434557743 -2.7867616398 2.117106794
 C -3.8679048946 -1.1918072559 0.9131538972
 C -2.7126683966 -0.6040943 0.4231601418
 N -1.4965181018 1.1130871396 -0.7193741416
 C -1.3662465777 2.1709495914 -1.5370547807
 C 0.0083604559 2.6383955518 -1.8973706054
 H -0.0453484135 3.4379755353 -2.6316288874
 H 0.5453153777 3.014076007 -1.0270967091
 H 0.5927288051 1.8211588878 -2.3216606899
 N -1.4966066236 -1.113004701 0.7193379503
 C -1.3664230989 -2.1708668542 1.5370357293
 C 0.0081427329 -2.6383779127 1.8974249771
 H 0.5925305029 -1.8211674587 2.321739181
 H 0.5451230467 -3.0140921774 1.0271824514
 H -0.0456431026 -3.437948644 2.6316876105
 C -2.5004160553 2.7950085251 -2.0487818038
 H -2.3857348338 3.6493878117 -2.6991738197
 C -3.7554330611 2.3097069428 -1.7264179681
 H -4.6432244337 2.7870477535 -2.1172212174
 C -3.8678058095 1.1920354353 -0.9132587788
 C -2.7126191904 0.6042500248 -0.4232342072
 H -4.8383229567 0.7849809917 -0.6795387906
 H 4.8383830284 0.7846837446 0.6794473234
 C 2.5006218517 2.7948570404 2.048726276
 H 2.3860042602 3.6492442969 2.6991190402

C 3.7556035988 2.3094773881 1.7263418647
 H 4.6434308366 2.7867641868 2.1171295875
 C 3.8678945646 1.1917975365 0.9131830473
 C 2.712664026 0.604081037 0.4231793645
 N 1.4965251518 -1.1130980443 -0.7193723299
 C 1.3662639271 -2.1709495454 -1.5370704372
 C -0.0083360763 -2.6383788153 -1.897435874
 H 0.0453895704 -3.4379429726 -2.6317101617
 H -0.5453185165 -3.0140757644 -1.0271870341
 H -0.5926873143 -1.8211302224 -2.3217264074
 N 1.4965995457 1.1129937222 0.7193398609
 C 1.3664057196 2.1708667689 1.5370202517
 C -0.0081671476 2.6383944104 1.8973599923
 H -0.5925719215 1.8211958358 2.321673802
 H -0.5451200568 3.0140921194 1.0270924575
 H 0.0456018905 3.4379809798 2.6316066122
 C 2.5004401471 -2.795003395 -2.0487885735
 H 2.3857668137 -3.6493708686 -2.6991975043
 C 3.7554533523 -2.3097092145 -1.7263997932
 H 4.6432493388 -2.7870451209 -2.1171985496
 C 3.8678161184 -1.1920451339 -0.9132296579
 C 2.712623542 -0.6042632647 -0.4232150209
 H 4.8383303684 -0.7849915148 -0.6794961809
 Cu -0.0000000073 -0.0000074156 0.0000131746

- ***Cull-BPA-OH.xyz:***

55
 Cull-BPA-OH
 H 4.9391631766 0.3199268773 0.0357507854
 C 3.4363115017 -2.3148466667 1.5089252677
 H 3.6466488947 -3.2535471667 2.0004848736
 C 4.4608438397 -1.5032360196 1.0522141794
 H 5.4931523908 -1.7984762573 1.1813865512
 C 4.1524232634 -0.3107647467 0.4178151932
 C 2.8178221036 0.0439991835 0.2598606308
 N 1.1087783555 1.3308866414 -0.8193712866
 C 0.6665971857 2.3289011356 -1.5902154074
 C -0.7638208276 2.2935379769 -2.0377922349
 H -0.864920083 2.7484576503 -3.0222091414
 H -1.1249328582 1.2688641628 -2.0761795188
 H -1.4051069091 2.851655808 -1.353606564
 N 1.8356087745 -0.7552016372 0.7158638207
 C 2.1152730332 -1.9161765412 1.3288161614
 C 0.9697164669 -2.7605373368 1.7907091985
 H 0.435928163 -3.181734979 0.9362769919
 H 0.2640975858 -2.151397636 2.3562564888
 H 1.3207615292 -3.5829016845 2.4097673704
 C 1.5204223883 3.3604752629 -1.9832654857
 H 1.1447428395 4.159871199 -2.6065152005
 C 2.8411140715 3.3402913421 -1.5706306123

H 3.5155877743 4.1383121933 -1.8499507502
 C 3.3011378111 2.2727085796 -0.8127353855
 C 2.4036743844 1.269446831 -0.4662871058
 H 4.3331536978 2.2333290908 -0.5012076991
 H -4.1692602149 -2.4138541172 -0.7597963563
 C -1.2037097827 -3.2715331142 -2.1087605586
 H -0.7367433534 -4.0040569798 -2.751667875
 C -2.5422383745 -3.3673298017 -1.7764133625
 H -3.1410878373 -4.1926035063 -2.136710242
 C -3.1188539349 -2.3734483622 -1.0000605344
 C -2.3204224173 -1.3318739507 -0.5476127785
 N -1.9678517751 0.7250417646 0.6387044795
 C -2.3635982589 1.8757468653 1.2052832649
 C -1.3251698868 2.8589183025 1.6397589587
 H -1.7866278101 3.704550308 2.1447165648
 H -0.6125395068 2.3585810805 2.2952475835
 H -0.7705414324 3.2348707421 0.7780746332
 N -0.9978124914 -1.2915709826 -0.8102714943
 C -0.4444936667 -2.2121259983 -1.6115527754
 C 0.9970280612 -2.0711424699 -1.991880566
 H 1.6446054822 -2.6053818284 -1.2953087139
 H 1.2905900645 -1.0254275198 -1.9974267378
 H 1.162429122 -2.4957919869 -2.980762524
 C -3.7220548318 2.1451263575 1.3629451137
 H -4.0268591048 3.0755609053 1.8195262459
 C -4.6597258818 1.2239008986 0.9319775981
 H -5.7166170992 1.4183494808 1.0535759903
 C -4.2321551664 0.0550193944 0.3225829225
 C -2.8681449678 -0.1647264581 0.1808149923
 H -4.9508259148 -0.6566870995 -0.0506762413
 Cu -0.0584549148 0.0042282265 0.6303730585
 O 0.0376838828 0.3254335012 2.5216115634
 H 0.9500061458 0.2373701975 2.8157836023

- ***Cull-BPA-OOH.xyz:***

56

Cull-BPA-OOH

H 2.8789739965 0.5286703131 -3.4573101653
 C 3.3807088117 -1.7591398037 -1.0322686181
 H 4.0580759431 -2.5421934348 -0.7236625633
 C 3.6043737277 -1.0371420604 -2.1926453208
 H 4.4631221036 -1.2511660874 -2.8142905144
 C 2.7182832755 -0.0345986035 -2.5521600679
 C 1.6211291636 0.2192005546 -1.7364455923
 N -0.4953992224 1.2693444303 -1.2957179316
 C -1.5071879692 2.0952976296 -1.5795417894
 C -2.74185237 2.0147487937 -0.7332302846
 H -3.6307073266 2.1930060486 -1.3373285184
 H -2.8196277197 1.0387096407 -0.2606146944
 H -2.7253487009 2.7730290235 0.0519679072

N 1.4139009962 -0.5021524662 -0.6237960275
 C 2.2651194034 -1.466445376 -0.2531811213
 C 1.973150915 -2.2050691584 1.015082115
 H 1.0725387048 -2.8124017925 0.9097857688
 H 1.8054614691 -1.4948964045 1.8256207615
 H 2.7978775056 -2.8626395374 1.2804569985
 C -1.4186856521 2.9966675187 -2.6406404302
 H -2.2474115823 3.6567002932 -2.8554171919
 C -0.2665528821 3.0269366644 -3.4058191165
 H -0.1702743083 3.7257823587 -4.2257059341
 C 0.7606039293 2.1370291673 -3.1258408853
 C 0.6085488789 1.2542709371 -2.0631544265
 H 1.6553918763 2.1399509311 -3.7276913726
 H -2.9165658894 -3.1642362939 2.9848170354
 C -1.9775839369 -3.7573961334 -0.1956969692
 H -1.9945579025 -4.5162140949 -0.9650284406
 C -2.4856565915 -4.0107064087 1.0646797015
 H -2.8911024751 -4.9829449999 1.3093293466
 C -2.4960709403 -2.9931107474 2.006833577
 C -1.9627357184 -1.7587653513 1.6626755942
 N -1.4049373618 0.5310127272 2.1216487336
 C -1.5180991309 1.6855098082 2.7915922863
 C -0.8798682847 2.9276264301 2.2518651164
 H -1.5405605577 3.7799965383 2.4112144199
 H 0.0577997341 3.1242889117 2.7720861994
 H -0.6641699264 2.8361843697 1.192106466
 N -1.4026037479 -1.5451569965 0.4540589279
 C -1.4360806293 -2.5039285911 -0.4816002142
 C -0.8997846672 -2.207418711 -1.8474562518
 H 0.1513338026 -2.4892296946 -1.9243993459
 H -0.9865152956 -1.1488297413 -2.0738720471
 H -1.4479359668 -2.78063847 -2.5936074217
 C -2.2457320779 1.7397882301 3.9806662675
 H -2.3315578615 2.6806595173 4.5054399877
 C -2.8502333352 0.5966609537 4.4671244995
 H -3.4112511686 0.6221456296 5.3912799007
 C -2.7549104479 -0.5817420855 3.7414824461
 C -2.0302523691 -0.5818220925 2.5585133423
 H -3.2564139891 -1.4718926445 4.0857853046
 Cu -0.1025884797 0.1456497026 0.5947359013
 O 1.2703439853 1.0792747739 1.6223211231
 O 2.1092205811 1.9101895055 0.8019224197
 H 1.6833319982 2.7769384719 0.8786223323

- **Cul-BPB.xyz:**

53
 Cul-BPB
 C -0.0251739096 0.2182369126 2.8727090163
 C 0.4002917574 2.9505814691 3.2082221097
 C 0.2704489027 2.1171982658 4.3302557785

C 0.0578993179 0.7518854919 4.1667269941
 H -0.0377904338 0.1110001915 5.0420778232
 N -0.2544962982 -1.5857575432 1.2965401194
 C -0.4506486436 -2.8677148236 0.9634206807
 C 0.6286722394 4.4305223543 3.3365890891
 H 0.3373991051 2.539328688 5.3358946687
 N 0.1002920262 1.0177946956 1.7928765472
 C 0.3049767891 2.3308413288 1.9568533903
 C -0.2483354554 -1.2236341451 2.5964961737
 C -0.6554570529 -3.88928849 1.8980509876
 C -0.6496992382 -3.5105826804 3.2496775464
 C -0.4467256475 -2.1800527003 3.6025135561
 H -0.4476731027 -1.8931797077 4.6531482096
 C -0.8683323672 -5.3142824817 1.4703396687
 H -0.8061316286 -4.2607415875 4.0286358259
 H 0.3978248022 2.9212835587 1.0416676822
 H -0.4440681714 -3.0933278107 -0.1060963585
 H -0.2011957497 4.909957073 3.8804610576
 H -1.8351162028 -5.6945037714 1.837411071
 H 0.715551607 4.910924207 2.3521474709
 H -0.0841765097 -5.9692121695 1.8833127403
 H 1.5506457758 4.6381162904 3.9030650285
 H -0.8544837998 -5.4120367243 0.3759390212
 C 0.8756986161 0.4610044453 -2.7058439754
 C 3.6397383643 0.2728565376 -2.4159449531
 C 3.083379184 0.5588041588 -3.6725440658
 C 1.7032097919 0.6536525938 -3.8213183055
 H 1.2791081153 0.8798051622 -4.7986194475
 N -1.2564496598 0.3804661266 -1.5928525297
 C -2.5937389395 0.4392149158 -1.5603948303
 C 5.1239531331 0.1591959927 -2.2084631022
 H 3.7339866196 0.708964405 -4.5374997047
 N 1.4088731669 0.1868794747 -1.4968529897
 C 2.7378355419 0.0971883372 -1.3601073869
 C -0.6058572542 0.5430416344 -2.7638979279
 C -3.387788832 0.6648490938 -2.6907353883
 C -2.7093857787 0.8326938545 -3.9080842366
 C -1.3198798672 0.7724475862 -3.9486842739
 H -0.8007655756 0.8995920243 -4.8976210042
 C -4.8867315258 0.7244462659 -2.5986450518
 H -3.2719425725 1.0099798508 -4.8279128949
 H 3.104019226 -0.1270545459 -0.354906214
 H -3.0578429842 0.2991372231 -0.5807016155
 H 5.547296137 -0.6435424905 -2.833526333
 H -5.3508590189 -0.0354208243 -3.2476100559
 H 5.3678465079 -0.0590347034 -1.1594873269
 H -5.2614179218 1.7064973216 -2.9296720672
 H 5.6330731627 1.0941775233 -2.4924608265
 H -5.2335022462 0.5550005157 -1.5698113599
 Cu 0.0001451361 0.000048596 -0.0000003572

- **Cull-BPB.xyz:**

53
Cull-BPB
C -0.0251739096 0.2182369126 2.8727090163
C 0.4002917574 2.9505814691 3.2082221097
C 0.2704489027 2.1171982658 4.3302557785
C 0.0578993179 0.7518854919 4.1667269941
H -0.0377904338 0.1110001915 5.0420778232
N -0.2544962982 -1.5857575432 1.2965401194
C -0.4506486436 -2.8677148236 0.9634206807
C 0.6286722394 4.4305223543 3.3365890891
H 0.3373991051 2.539328688 5.3358946687
N 0.1002920262 1.0177946956 1.7928765472
C 0.3049767891 2.3308413288 1.9568533903
C -0.2483354554 -1.2236341451 2.5964961737
C -0.6554570529 -3.88928849 1.8980509876
C -0.6496992382 -3.5105826804 3.2496775464
C -0.4467256475 -2.1800527003 3.6025135561
H -0.4476731027 -1.8931797077 4.6531482096
C -0.8683323672 -5.3142824817 1.4703396687
H -0.8061316286 -4.2607415875 4.0286358259
H 0.3978248022 2.9212835587 1.0416676822
H -0.4440681714 -3.0933278107 -0.1060963585
H -0.2011957497 4.909957073 3.8804610576
H -1.8351162028 -5.6945037714 1.837411071
H 0.715551607 4.910924207 2.3521474709
H -0.0841765097 -5.9692121695 1.8833127403
H 1.5506457758 4.6381162904 3.9030650285
H -0.8544837998 -5.4120367243 0.3759390212
C 0.8756986161 0.4610044453 -2.7058439754
C 3.6397383643 0.2728565376 -2.4159449531
C 3.083379184 0.5588041588 -3.6725440658
C 1.7032097919 0.6536525938 -3.8213183055
H 1.2791081153 0.8798051622 -4.7986194475
N -1.2564496598 0.3804661266 -1.5928525297
C -2.5937389395 0.4392149158 -1.5603948303
C 5.1239531331 0.1591959927 -2.2084631022
H 3.7339866196 0.708964405 -4.5374997047
N 1.4088731669 0.1868794747 -1.4968529897
C 2.7378355419 0.0971883372 -1.3601073869
C -0.6058572542 0.5430416344 -2.7638979279
C -3.387788832 0.6648490938 -2.6907353883
C -2.7093857787 0.8326938545 -3.9080842366
C -1.3198798672 0.7724475862 -3.9486842739
H -0.8007655756 0.8995920243 -4.8976210042
C -4.8867315258 0.7244462659 -2.5986450518
H -3.2719425725 1.0099798508 -4.8279128949
H 3.104019226 -0.1270545459 -0.354906214
H -3.0578429842 0.2991372231 -0.5807016155
H 5.547296137 -0.6435424905 -2.833526333
H -5.3508590189 -0.0354208243 -3.2476100559

H 5.3678465079 -0.0590347034 -1.1594873269
 H -5.2614179218 1.7064973216 -2.9296720672
 H 5.6330731627 1.0941775233 -2.4924608265
 H -5.2335022462 0.5550005157 -1.5698113599
 Cu 0.0001451361 0.000048596 -0.0000003572

- ***CuI-BPC.xyz:***

57
 Cul-BPC
 C -1.6267093212 0.0502017969 1.8270017839
 C -0.4772920216 -1.5148308615 3.7918098756
 C -1.6265734431 -0.7817469536 4.0785200657
 C -2.2168406166 0.0135350669 3.0941852061
 H -3.1170143521 0.5834775107 3.3153327131
 N -1.5021696692 0.7342581727 -0.4690922342
 C -1.8998552203 1.4164142025 -1.545138344
 H -0.0110574247 -2.1367395618 4.5531660038
 H -2.0655549983 -0.83160477 5.0768773138
 N -0.5142468699 -0.6606255948 1.5516950545
 C 0.0501883786 -1.4210247943 2.4922141847
 C -2.1653198798 0.8565982074 0.6987710581
 C -3.009736697 2.2784921519 -1.5139492215
 C -3.6961906586 2.4067727118 -0.308633002
 C -3.2796665409 1.6930334191 0.816928237
 H -3.8122599067 1.795374171 1.7602861529
 H -3.3279055673 2.8309223467 -2.3956510062
 H -4.5620315543 3.0688641642 -0.2464838727
 O 1.1478873927 -2.0689882425 2.0712365882
 O -1.1430936305 1.1942305423 -2.6314022836
 C 1.7948094313 -2.0755038583 -2.2154305589
 C 0.1424148932 -4.2480794914 -2.640193989
 C 1.3961188854 -4.2063513982 -3.2459596053
 C 2.2404647931 -3.1135080462 -3.0396199114
 H 3.2218135074 -3.0813573335 -3.5086373495
 N 2.0439452798 0.0126910567 -1.0609383399
 C 2.6845711308 1.1354019525 -0.7285458605
 H -0.5215861991 -5.095804775 -2.7959977646
 H 1.7173304311 -5.0326351459 -3.8831301041
 N 0.5807749508 -2.1182551092 -1.629823006
 C -0.2265522099 -3.1626896209 -1.8266985722
 C 2.6050796952 -0.8635941217 -1.9187791783
 C 3.9525474546 1.452169231 -1.2461193544
 C 4.5341126686 0.5486867171 -2.1326667482
 C 3.8634690585 -0.6257243636 -2.4802292205
 H 4.3144960873 -1.3304493831 -3.1759255329
 H 4.4685236001 2.3694007645 -0.969961161
 H 5.5173789955 0.762452968 -2.5562224899
 O -1.398472593 -3.064713443 -1.1793801881
 O 2.0025173838 1.9079662524 0.1316697439
 Cu 0.1520911598 -0.5080359191 -0.4020006782

C 1.8538369281 -2.91807637 2.9716390877
 C -1.4529608085 1.8573285041 -3.8538265961
 C -2.3592330436 -4.1100138165 -1.2990666827
 C 2.5671791376 3.1392894439 0.573300419
 H 2.6965442872 -3.3263469824 2.4027339649
 H -3.2157531665 -3.80339709 -0.688449379
 H -0.7041284711 1.5187909464 -4.5784893808
 H 1.8325308946 3.5798290124 1.2564627871
 H 2.736612232 3.8231982969 -0.2733966635
 H 1.2136677631 -3.7433489062 3.3215587025
 H -1.9582065858 -5.0618563752 -0.9163033081
 H -1.3842432138 2.9507277625 -3.7394128968
 H 2.2352386387 -2.3500436468 3.8349254498
 H -2.6807367415 -4.2345223817 -2.3452619262
 H -2.4583485117 1.5820079587 -4.2098972577
 H 3.5133008279 2.9705944071 1.1116206281

- ***Cull-BPC.xyz:***

57
 Cull-BPC
 C -1.7178579815 -0.1116177472 1.7098143217
 C -0.9907255464 -2.1995596067 3.3696556782
 C -2.047726657 -1.3692940381 3.7224006853
 C -2.4183483488 -0.3012127815 2.8968155162
 H -3.232568219 0.3620022254 3.181295532
 N -1.2072491935 0.9656040132 -0.3589156897
 C -1.3789220651 1.863052391 -1.3384257978
 H -0.686535059 -3.0209408866 4.0147619763
 H -2.5847967123 -1.5460807694 4.6559747809
 N -0.7064640456 -0.9398756142 1.3578751704
 C -0.318766185 -1.9387095076 2.1618390795
 C -1.9894094749 0.9785532738 0.7460176501
 C -2.3355506545 2.8877671174 -1.2233118696
 C -3.1222801374 2.9222710547 -0.0783757942
 C -2.9654571828 1.9544436144 0.9208584255
 H -3.5943383682 1.9680298011 1.8085889344
 H -2.463747108 3.6266228632 -2.0113604217
 H -3.8752122335 3.7041160048 0.0359482011
 O 0.7338824165 -2.6148611237 1.7125838451
 O -0.586070516 1.6735322895 -2.3884528756
 C 1.8571726266 -2.1258782278 -2.0108629589
 C 0.5237771485 -4.5397933864 -1.8154100043
 C 1.703431537 -4.4565359971 -2.5451337612
 C 2.3820137325 -3.2376819239 -2.6620455842
 H 3.2948677308 -3.1661946939 -3.2496913629
 N 1.8002875689 0.1612947677 -1.328000543
 C 2.2617994412 1.4153725716 -1.2350638433
 H -0.0176111815 -5.4798593468 -1.7345653616
 H 2.096521168 -5.3467609909 -3.0393384949
 N 0.7221190309 -2.21865264 -1.2788403948

C 0.0446703688 -3.371280171 -1.1961688799
 C 2.457739435 -0.7736171215 -2.0535998205
 C 3.4103860603 1.8192093015 -1.9393804276
 C 4.0734178321 0.8702558104 -2.7080784012
 C 3.6084825671 -0.4489706755 -2.764933432
 H 4.1378877705 -1.1980043661 -3.3500969474
 H 3.7759213236 2.841890344 -1.8771683468
 H 4.9696333778 1.1547743194 -3.2622493595
 O -1.0868509039 -3.283271996 -0.5040648967
 O 1.5487783236 2.1938451324 -0.4271943789
 Cu 0.1526480216 -0.5076047301 -0.4015630283
 C 1.2295597026 -3.7421409915 2.438905091
 C -0.6201385197 2.5836345846 -3.4905158666
 C -1.8910363224 -4.4452890637 -0.2872996108
 C 1.8908834161 3.5729223698 -0.2687269278
 H 2.0614096416 -4.1342304663 1.8446135053
 H -2.7307225291 -4.1124623621 0.3316059618
 H 0.1419842212 2.2277351086 -4.1915118643
 H 1.1370553805 3.9886734661 0.4078715432
 H 1.8507204662 4.0975211999 -1.2348122567
 H 0.4512846819 -4.5129826958 2.5400325134
 H -1.3208481985 -5.2191392527 0.2476555743
 H -0.3725074134 3.6035540907 -3.1610006209
 H 1.5937714118 -3.4365538716 3.4310675054
 H -2.2677291713 -4.8417510032 -1.2419398876
 H -1.607033332 2.5697905086 -3.9765829533
 H 2.8901028281 3.677181207 0.179722526

- ***Cul-BPD.xyz:***

41
 Cul-BPD
 H -3.1630232732 3.7883148621 -1.0547103415
 C -4.2879749292 0.803915549 0.1097737404
 H -5.1955766462 0.2606569785 0.3760455197
 C -4.3335202644 2.1186620405 -0.3592780377
 H -5.2869732284 2.6379993291 -0.4730935099
 C -3.1413114368 2.7647908068 -0.6839162854
 C -1.9272252049 2.0811197966 -0.5322436878
 N 0.4663851496 1.8829858352 -0.7028028696
 C 1.6907255104 2.3547207226 -0.9714386584
 H 2.5203382543 1.6579991206 -0.8323576934
 N -1.8966075243 0.80833285 -0.0789852784
 C -3.0424643526 0.1889158729 0.2325418517
 H -2.9559729646 -0.8381116724 0.5941414542
 C 1.9154772077 3.6603849245 -1.4065511556
 H 2.9305854719 4.001357943 -1.6140702451
 C 0.8138198843 4.5042173616 -1.5644774992
 H 0.9436350728 5.5346390244 -1.9008063152
 C -0.4614513548 4.0143811 -1.2852313206
 C -0.6078311397 2.6890566018 -0.8533688764

H -1.3284228897 4.6630105853 -1.4001293525
 H 2.4670880352 -3.8384648796 2.1559372841
 C 1.77826131 -0.9847039528 3.861734677
 H 1.9061955981 -0.4976016256 4.8292756564
 C 2.2748272374 -2.2669655934 3.6170517972
 H 2.8088772786 -2.8165109638 4.3945658902
 C 2.0813401016 -2.841160522 2.3612265315
 C 1.394303043 -2.119528023 1.3755072341
 N 0.510474043 -1.8126501728 -0.8431386236
 C 0.2455025289 -2.2152856288 -2.0926915552
 H -0.2653482042 -1.4956042347 -2.736207002
 N 0.920123461 -0.8786884662 1.6241805948
 C 1.1065942654 -0.328372248 2.8308685031
 H 0.7011315424 0.6756811552 2.9740371348
 C 0.5948282437 -3.4796022975 -2.5660522315
 H 0.3593648584 -3.7644208393 -3.5923109511
 C 1.2457216463 -4.3559020877 -1.6948007046
 H 1.5354961377 -5.3561030418 -2.0224692329
 C 1.5222867939 -3.9379985786 -0.3936077328
 C 1.1413764599 -2.6506516846 0.0089623207
 H 2.0254223505 -4.6128343931 0.2970533023
 Cu 0.0000195854 -0.0000066018 -0.0000569326

- *Cull-BPD.xyz:*

41

Cull-BPD

H -4.2664908092 2.3900630983 -0.9689627169
 C -3.2519779267 1.7177751105 2.2064985708
 H -3.5193211348 1.8618182671 3.2534894007
 C -4.0543108567 2.2009386642 1.1720567685
 H -4.9797100719 2.7364100421 1.3909722646
 C -3.6591010678 2.0034226724 -0.1523199075
 C -2.4718861383 1.3163048211 -0.4118275244
 N -0.7166785653 0.4788593915 -1.8075395849
 C -0.1494675262 0.1683041808 -2.9798481678
 H 0.8212429348 -0.3276557176 -2.9434598859
 N -1.7161592453 0.8365008725 0.604353369
 C -2.0812363184 1.0377794467 1.8766296868
 H -1.4163638667 0.6495062143 2.6491373433
 C -0.7683733081 0.4558319266 -4.1948079982
 H -0.2764353224 0.1903689408 -5.1307230628
 C -2.0158482066 1.0808383725 -4.174122015
 H -2.5305509336 1.3239175803 -5.1052562224
 C -2.6101579151 1.3859909101 -2.9482121279
 C -1.9359920508 1.0668055356 -1.7681377779
 H -3.5908034749 1.8578759935 -2.9169501014
 H 4.5578935902 -1.4955430926 1.3576440926
 C 4.0656350503 0.7799284462 -1.1212009485
 H 4.5905283499 1.4264953149 -1.8246559426
 C 4.7534088435 -0.0549023034 -0.2395662035

H 5.8444072603 -0.0820293165 -0.2375964676
C 4.034059928 -0.8524068534 0.6524542837
C 2.6389849736 -0.8033624681 0.634706942
N 0.4449784729 -1.3129113129 1.4451241986
C -0.4418088899 -1.9833693948 2.1911633821
H -1.4949973245 -1.7405939171 2.0447621256
N 1.9878764924 -0.0024067755 -0.2419265402
C 2.6725343228 0.7773422061 -1.0879268572
H 2.0901690561 1.4188914443 -1.7503804913
C -0.045294571 -2.9535799111 3.1094835382
H -0.794778032 -3.4787121642 3.7018695989
C 1.3167015126 -3.2270380131 3.2415514341
H 1.6657787438 -3.9785435864 3.9517639155
C 2.2351461482 -2.5371834541 2.4479915498
C 1.7688742179 -1.5798187889 1.5452192851
H 3.2993182354 -2.7526651338 2.5281412546
Cu 0.0000124011 0.0000358353 0.000014102

- 1 E. C. Constable and C. E. Housecroft, *Molecules*, 2019, **24**, 3951.
- 2 A. Prazeres, A. M. Santos, M. J. Calhorda, C. C. Roma and I. S. Gonçalves, *Chem. - A Eur. J.*, 2002, **8**, 2370–2383.
- 3 B. Bozic-Weber, V. Chaurin, E. C. Constable, C. E. Housecroft, M. Meuwly, M. Neuburger, J. A. Rudd, E. Schönhofe and L. Siegfried, *Dalt. Trans.*, 2012, **41**, 14157–14169.
- 4 P. J. Burke, D. R. Mcmillin and W. R. Robinson, *Inorg. Chem.*, 1980, **19**, 1211–1214.
- 5 M. Munakata, S. Kitagawa, A. Asahara and H. Masuda, *Bull. Chem. Soc. Jpn.*, 1987, **60**, 1927–1929.
- 6 D. Dhar, G. M. Yee, A. D. Spaeth, D. W. Boyce, H. Zhang, B. Dereli, C. J. Cramer and W. B. Tolman, *J. Am. Chem. Soc.*, 2016, **138**, 356–368.
- 7 A. D. Spaeth, N. L. Gagnon, D. Dhar, G. M. Yee and W. B. Tolman, *J. Am. Chem. Soc.*, 2017, **139**, 4477–4485.
- 8 J. S. Woertink, L. Tian, D. Maiti, H. R. Lucas, R. A. Himes, K. D. Karlin, F. Neese, C. Würtele, M. C. Holthausen, E. Bill, J. Sundermeyer, S. Schindler and E. I. Solomon, *Inorg. Chem.*, 2010, **49**, 9450–9459.
- 9 R. L. Peterson, R. A. Himes, H. Kotani, T. Suenobu, L. Tian, M. A. Siegler, E. I. Solomon, S. Fukuzumi and K. D. Karlin, *J. Am. Chem. Soc.*, 2011, **133**, 1702–1705.
- 10 B. N. Sánchez-Eguía, M. Flores-Alamo, M. Orio and I. Castillo, *Chem. Commun.*, 2015, **51**, 11134–11137.
- 11 S. Paria, T. Ohta, Y. Morimoto, T. Ogura, H. Sugimoto, N. Fujieda, K. Goto, K. Asano, T. Suzuki and S. Itoh, *J. Am. Chem. Soc.*, 2015, **137**, 10870–10873.